Natural Sciences Tripos Part IB
Mineral Sciences
Module B:
Reciprocal Space, Symmetry and Crystallography

Dr Andrew L Goodwin
Michaelmas Term 2008

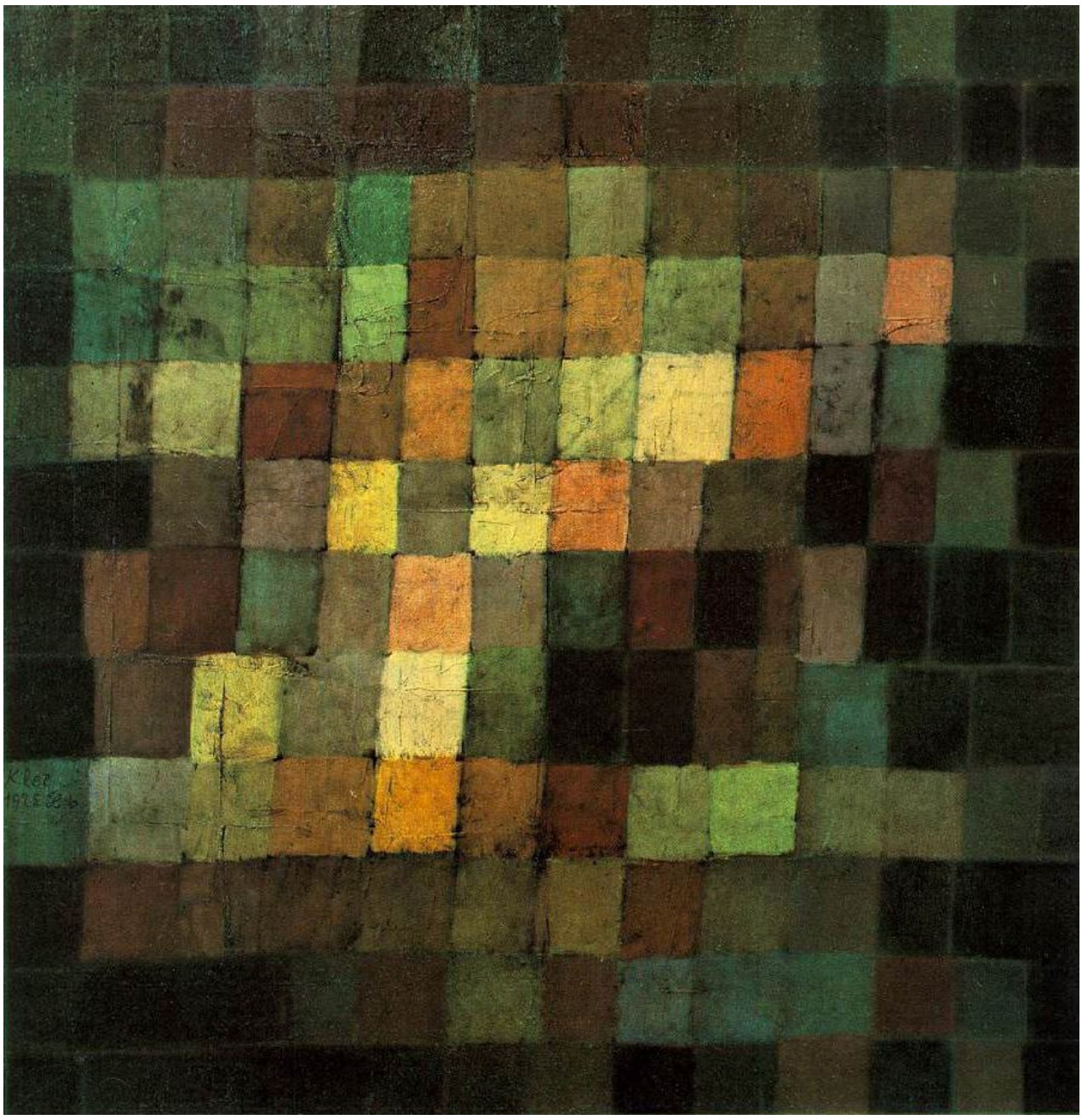

Contents

Cover picture: Ancient Sound, Paul Klee, 1925.

Synopsis of Module B lectures

BL1 (Thursday): Reciprocal Space
Introduction to reciprocal space. Fourier relationship between real space and reciprocal space. Convolution and the convolution theorem.

BL2 (Saturday): Periodicity
Lattice periodicity and the unit cell. Bravais lattices. Reciprocal lattice and reciprocal cell. Reciprocal space vectors.

BL3 (Tuesday): Diffraction Geometry
Relationship between reciprocal space formalism and Bragg scattering equations. Definition of the scattering vector.

BL4 (Thursday): Experimental Techniques
Beams of radiation: x-rays, neutrons and electrons. Thermal motion and the temperature factor. Convolution description of the structure factor. Patterson maps.

BL5 (Saturday): Point Symmetry
Introduction to point group symmetry. Sphere diagrams. Laue classes. Point symmetry of diffraction patterns.

BL6 (Tuesday): Translational Symmetry
Define and illustrate glide planes, screw axes and lattice centreing. Introduce space group diagrams (without formalism of space groups themselves).

BL7 (Thursday): Space Groups
Space group labels. Recognising symmetry elements. Constructing space group diagrams. Exercises.

BL8 (Saturday): Systematic Absences
Systematic absences due to translational symmetry elements. Orthorhombic space groups and observed reflection diagrams.

BL9 (Tuesday): The Phase Problem
Reminder of the phase problem. Introduction to direct methods. Solution of crystal structures. Refinement of crystal structures.

Recommended reading list

Standard texts on crystallography and diffraction

M. T. Dove, *Structure and Dynamics* (Oxford University Press, 2003).
G. E. Bacon, *Neutron Diffraction* (Oxford University Press, 1975).
G. Harburn, C. A. Taylor & T. R. Welberry, *Atlas of optical transforms* (Bell, 1975).
M. F. C. Ladd & R. A. Palmer, *Structure determination by X-ray crystallography* (Plenum, 1985).
D. McKie & C. McKie, *Essentials of Crystallography* (Blackwell, 1986).
P. Luger, *Modern X-ray analysis on single crystals* (de Gruyter, 1980).

Books that present elements of crystallography in a "Mineral Sciences" context

A. Navrotsky, *Physics and Chemistry of Earth Materials* (Cambridge University Press, 1994).
A. Putnis, *Introduction to Mineral Sciences* (Cambridge University Press, 1992).
A. F. Wells, *Structural Inorganic Chemistry* (Clarendon Press, 1984).

You are encouraged to make use of the class library in the IB Mineral Sciences laboratory, and also the Departmental Library on the 2nd floor of the North Wing.

Useful websites

You should also look at the course WWW pages, which contain links to a number of relevant sites—e.g. tutorials and other information—and links to pages that describe the research of Cambridge Mineral Sciences group:

`http://rock.esc.cam.ac.uk/~alg44/teaching.html`
`http://www.esc.cam.ac.uk/ibminsci/IB_Min_Sci.html`

A particularly useful website for learning about reciprocal space is the "Diffraction and Fourier transform" Java applet written by Nicolas Schoeni and Gervais Chapuis:

`http://escher.epfl.ch/eCrystallography/applets/fft.html`

In addition, Kevin Cowtan has produced a very useful online "Book of Fourier", from which many of the cat/duck examples used in this course are taken:

`http://www.ysbl.york.ac.uk/~cowtan/fourier/fourier.html`

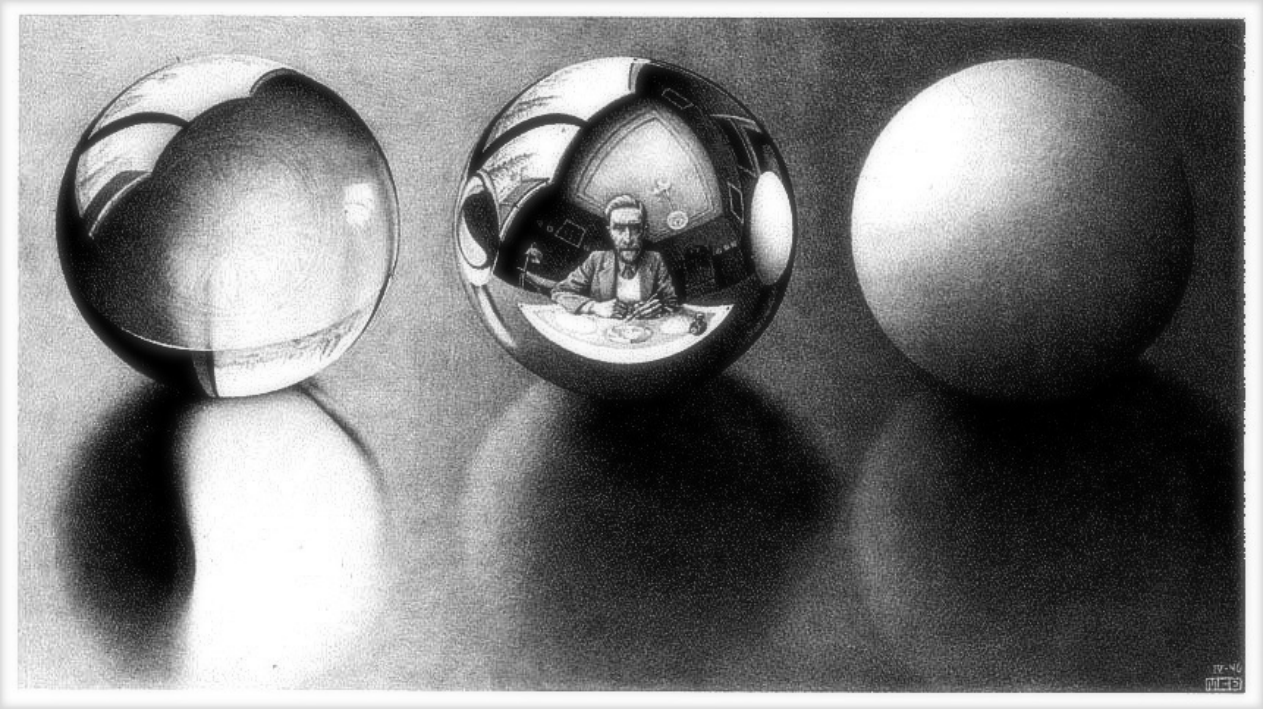

Three Spheres II, Maurits Escher, 1946

BL1: Reciprocal space

Our goal in this course is to explain how scientists have managed, over the past century, to determine the atomic-level structure of materials. The required resolution being so high, it is extremely difficult to build a microscope capable of looking directly at atoms and their arrangement in solids. And so the community has instead developed the indirect technique of diffraction — whereby one measures the interference patterns of radiation scattered from (usually crystalline) materials, and deduces from these patterns the arrangement of atoms within. It was the technique developed by the Braggs and which famously they used to discover how sodium and chlorine atoms are arranged in humble table salt, one that in turn allowed Watson, Crick and Franklin to determine the helical structure of DNA, and one that has given us since an "atomic-eye view" of the structure of nearly half a million compounds: minerals, materials, chemicals and biological molecules.

In order to understand how diffraction works, we need some idea of how waves interact with matter. And the key is to think of the arrangement of atoms in a material as a set of waves itself. A bizarre concept, surely. But actually atoms are small enough that the "particle-like" descriptions of structure we might instinctively seek to use — density at a given position in space — are no more real than the "wave-like" concepts of amplitude and periodicity. It would seem strange, for example, to describe a wave on a body of water in terms of a "mass", or to locate it at a precise point in space. The same is true of the radiation one uses in a diffraction experiment, and in some senses the same is true even of individual atoms. While our intuition lives in "real space", where structure is a density

function $\rho(\mathbf{r})$ that characterises how much matter is at a given point $\mathbf{r}$, what we will develop in this lecture is a feel for "reciprocal space", where structure is defined instead in terms of a function $F(\mathbf{Q})$ that tells us what components of waves of periodicity $\mathbf{Q}$ are required to produce the same arrangement of atoms.

Let us first formalise what we mean by periodicity. Here there are two concepts: a wave repeats after a given distance, called the wavelength λ, and a wave propagates along a particular direction. So by saying a wave has the periodicity $\mathbf{Q}$ we are defining $Q = |\mathbf{Q}| = 2\pi/\lambda$ and assigning the direction $\mathbf{Q}/Q$ to be the same as the direction of propagation of the wave. Mathematically, we would represent the wave by the function $\psi(\mathbf{r}) = \exp(\mathrm{i}\mathbf{Q}\cdot\mathbf{r})$. Note that this function repeats every time that $\mathbf{Q}\cdot\mathbf{r}$ increases by another multiple of 2π, which will occur for each wavelength λ added to $\mathbf{r}$ in a direction parallel to $\mathbf{Q}$. Conveniently, this is precisely what we mean by a wave of wavelength λ that propagates parallel to $\mathbf{Q}$.

A key point is that large values of Q correspond to waves with very small wavelengths, while small values of Q correspond to waves with long wavelengths. So, perhaps counterintuitively, as we add waves of larger and larger values of Q to assemble our material structure, we are actually making finer- and finer-scale adjustments in real space. The broadest features in real-space will be described by waves of smallest Q values in reciprocal space. Note also that the units of Q are inverse length (usually Å^{-1}, since we will be using Å as units for structure on the atomic scale). So when we speak of reciprocal space, we are using inverse lengths as our units.

The conversion itself between real space and reciprocal space is relatively straightforward. As we said above, our reciprocal space function $F(\mathbf{Q})$ is meant to tell us what components of waves of periodicity $\mathbf{Q}$ are needed to produce the real-space density function $\rho(\mathbf{r})$. This is precisely the mapping described by Fourier transforms, which tell us how to deconstruct any function into an equivalent set of waves of different periodicities. The mathematics gives us then:

$$F(\mathbf{Q}) = \int \rho(\mathbf{r}) \exp(\mathrm{i}\mathbf{Q}\cdot\mathbf{r})\,\mathrm{d}\mathbf{r}, \tag{1}$$

$$\rho(\mathbf{r}) = \frac{1}{2\pi}\int F(\mathbf{Q}) \exp(-\mathrm{i}\mathbf{Q}\cdot\mathbf{r})\,\mathrm{d}\mathbf{Q}. \tag{2}$$

We will see in BL3 that what diffraction does is to give us a way of measuring $F(\mathbf{Q})$ (or, at least, related functions). In principle, if we measure $F(\mathbf{Q})$ for sufficiently many values of $\mathbf{Q}$ then we could use the reverse Fourier transform (equation (2) above) to reconstruct the distribution function $\rho(\mathbf{r})$. This is the underlying idea of crystallography, and essentially the goal of this course. There are problems along the way (otherwise we wouldn't need nine lectures), and we will deal with these as we come to them. But for the time being what is most important is for us to develop an intuition for what $F(\mathbf{Q})$ looks like for different systems — how it is related to $\rho(\mathbf{r})$ and what it can tell us in itself about material structure.

Perhaps the first thing to note about $F(\mathbf{Q})$ is that it is a complex number (even given that the real-space distribution $\rho(\mathbf{r})$ is real, and positive, everywhere). As such, we can

think separately about its magnitude $|F(\mathbf{Q})|$ and its complex argument ϕ, which we call its "phase"; that is, $F(\mathbf{Q}) = |F(\mathbf{Q})| \times \exp(\mathrm{i}\phi)$. We will use a very convenient method of representing both of these components pictorially (see following figure), where a diagram of reciprocal space is coloured such that the intensity at a given point $\mathbf{Q}$ corresponds to the magnitude of $F(\mathbf{Q})$, and the colour tells us about the phase ϕ.

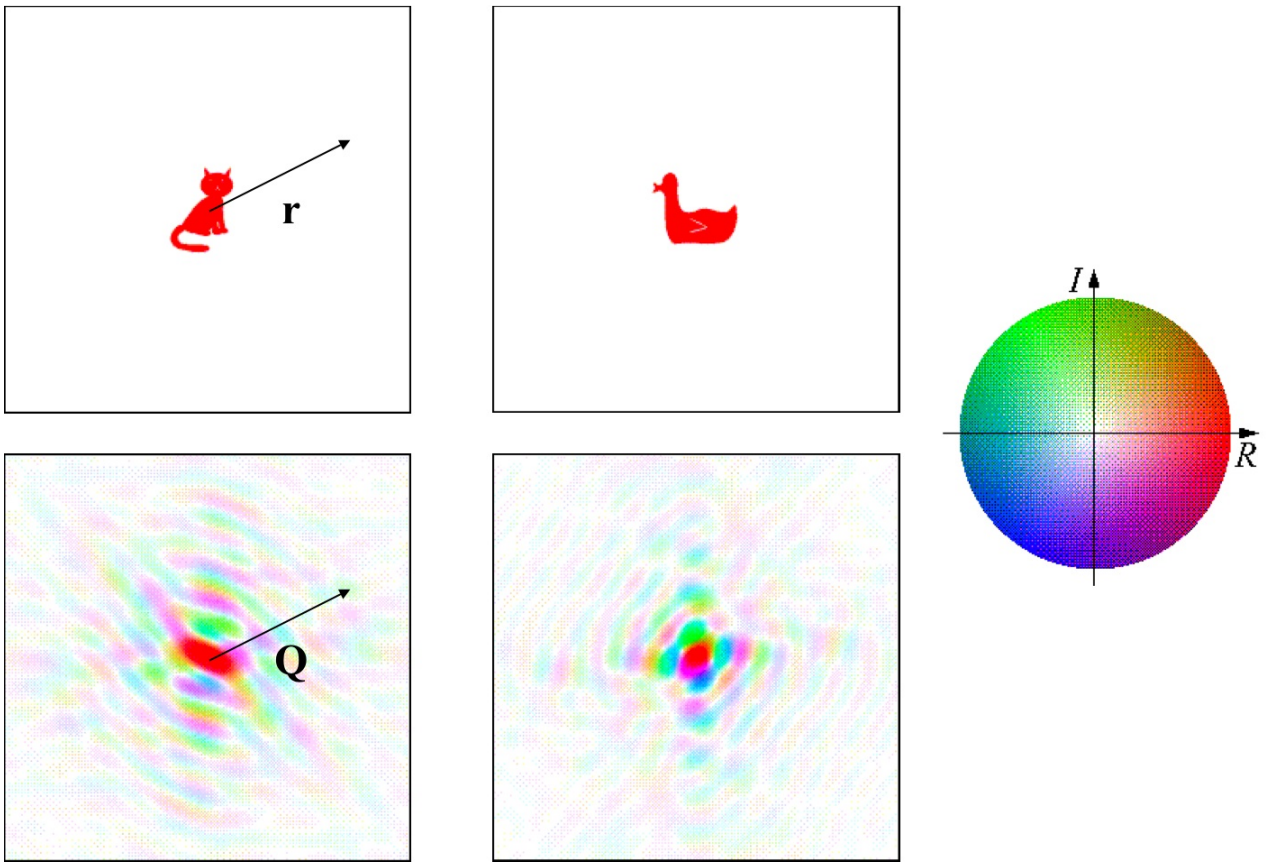

What we have done in this picture is to take the Fourier transform of an image of a cat and of an image of a duck. The real-space distribution functions have been simplified in each case such that $\rho(\mathbf{r})$ is either 1 (if some part of a duck or a cat indeed exists at the point $\mathbf{r}$) or 0 (if the point $\mathbf{r}$ is animal-less). Of course both $\mathbf{r}$ and $\mathbf{Q}$ are two-dimensional vectors in this case, but everything we notice will apply equally well to three dimensions. Let us make some observations:

(i) The Fourier transforms look neither like a cat nor like a duck.

(ii) In both cases, there is a "blob" near $\mathbf{Q} = 0$ that has the same phase ($\phi \sim 0$).

(iii) There is a kind of symmetry — despite the obvious lack of symmetry in real-space — in that the arm-like feature to the top-left of the cat Fourier transform is mirrored by a similar feature to the bottom-right, with the phases reversed between the two. The same type of relation can be seen throughout both patterns.

(iv) The magnitudes of $F(\mathbf{Q})$ tend to decrease with increasing Q.

Our first observation is reassuring, because it tells us that we do indeed need to think about Fourier transforms: they will rarely be obvious to us. Point (ii) also makes sense if we consider how equation (1) simpilfies as $\mathbf{Q} \rightarrow 0$: in this limit we obtain $F(0) = \int \rho(\mathbf{r})\,\mathrm{d}\mathbf{r}$, which is of course just the total density in the entire real space function — namely, the amount of cat or the amount of duck. Since both are positive and real, we expect a positive and real value for $F(0)$; hence the graphical Fourier transforms are intense and red-coloured at their centres. Our statement with regard to symmetry also follows from equation (1) if we consider the relationship between $F(\mathbf{Q})$ and $F(-\mathbf{Q})$:

$$F(-\mathbf{Q}) = \int \rho(\mathbf{r}) \exp(-\mathrm{i}\mathbf{r}\cdot\mathbf{Q})\,\mathrm{d}\mathbf{r} = \left[\int \rho(\mathbf{r}) \exp(\mathrm{i}\mathbf{Q}\cdot\mathbf{r})\,\mathrm{d}\mathbf{r}\right]^* = [\mathrm{F}(\mathbf{Q})]^*, \tag{3}$$

where the asterisk notation represents the operation of complex conjugation. Hence the magnitudes of $F(\mathbf{Q})$ and $F(-\mathbf{Q})$ are identical, and their phases reversed. This rule is known as “Friedel’s law”, which also demands that $F(0)$ must be real.

To understand the last of our four observations, we must recall our statements above concerning the meaning of $F(\mathbf{Q})$ at large Q. The bulk of the density in real space — the fact that, for either cat or duck, we basically have a collection of density near the origin and not much else — will be recovered from the long-wavelength information near $\mathbf{Q} = 0$. The high-frequency information at larger Q will help separate the cat’s tail from its body, or will give the duck its beak and wings. This sort of detail concerns less and less density in real space, and so the components of the waves required will decrease with increasing Q.

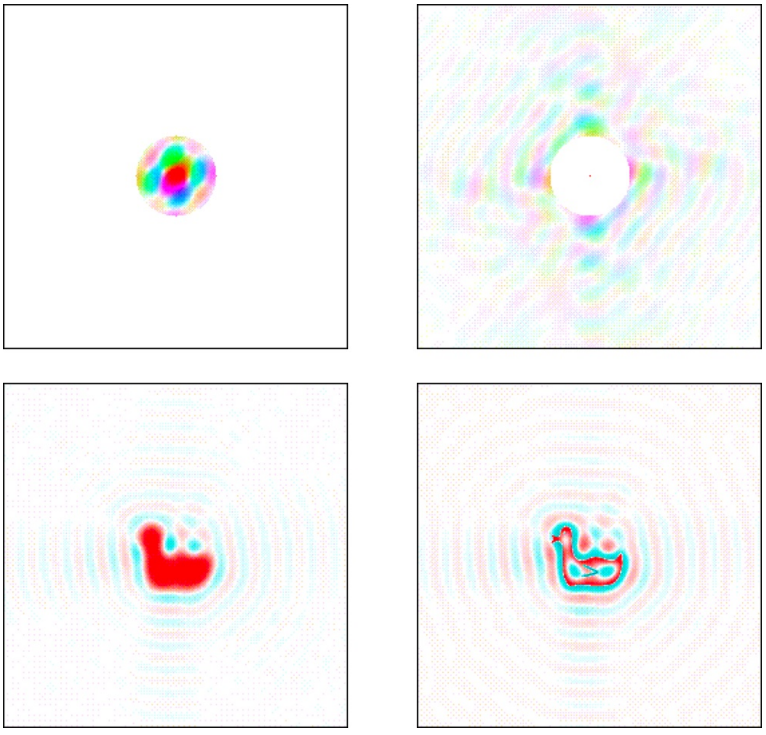

In the picture above we have illustrated this by calculating the reverse Fourier transform of the duck image with different parts of reciprocal space excluded. If we use just the low Q

region (left hand side in the image above), then we get the broad features of the duck; if we use just the high Q region, then we obtain the edges. Indeed these approaches are used in image processing for compression (low Q filtering) or to determine edges (high Q).

The final concept we are going to deal with in this lecture is called convolution and is a little strange. It is the idea of combining two functions such that we place a copy of one function at each point in space, weighted by the value of the second function at the same point. The mathematics is dealt with separately in an appendix, but the concept (which is all that is important) is explained more satisfactorily through a diagram.

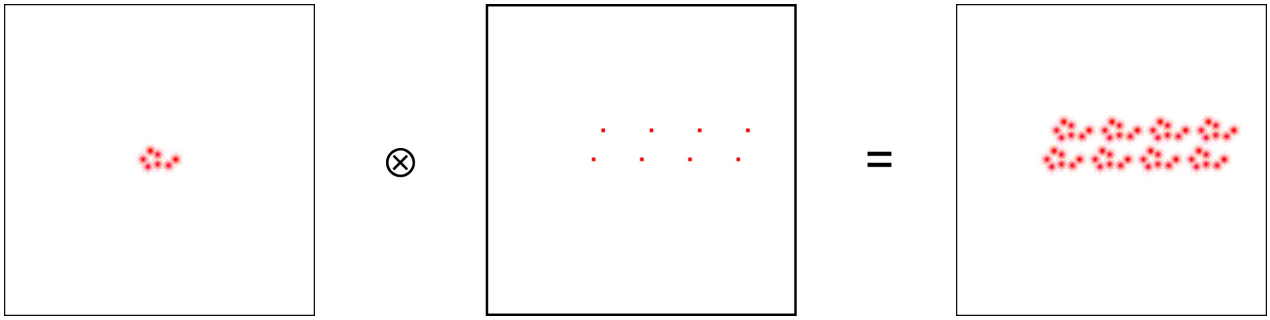

On the left hand side we have two density functions: the first might reasonably represent a single molecule, while the second is just a set of points. What the convolution of these two functions does is to place a copy of the molecule at each point in the set (or, equivalently, to copy the set of points for each atom in the molecule). We end up with a set of molecules, whose spacing is determined by the original set of points. The convolution operation itself is represented by the operator $\otimes$, and is quite useful because it enables us to deconstruct a complex object (a group of molecules) into two simpler objects: a single molecule and an array of points. But it is even more useful in the current context, because the Fourier transform of a convolution is equivalent to the product of the individual Fourier transforms. Let us see this pictorially in terms of the Fourier transforms of the above images:

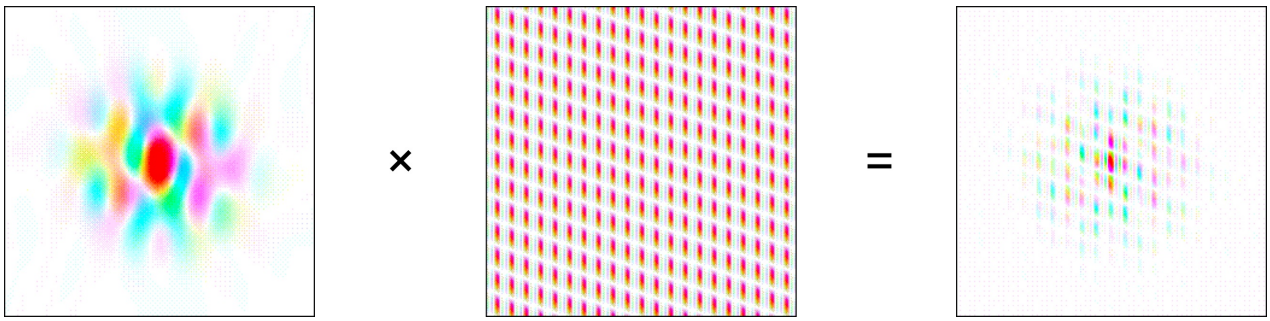

Note that the Fourier transform of the grid of points is itself real-valued everywhere, so that the phases in the final result come directly from the phases for the individual molecule. So on the one hand the phases are telling us something about the molecule, while on the other hand grid-like intensity is telling us about how the molecules are repeated in real space. The importance of periodicity now forms the subject of our next lecture, BL2.

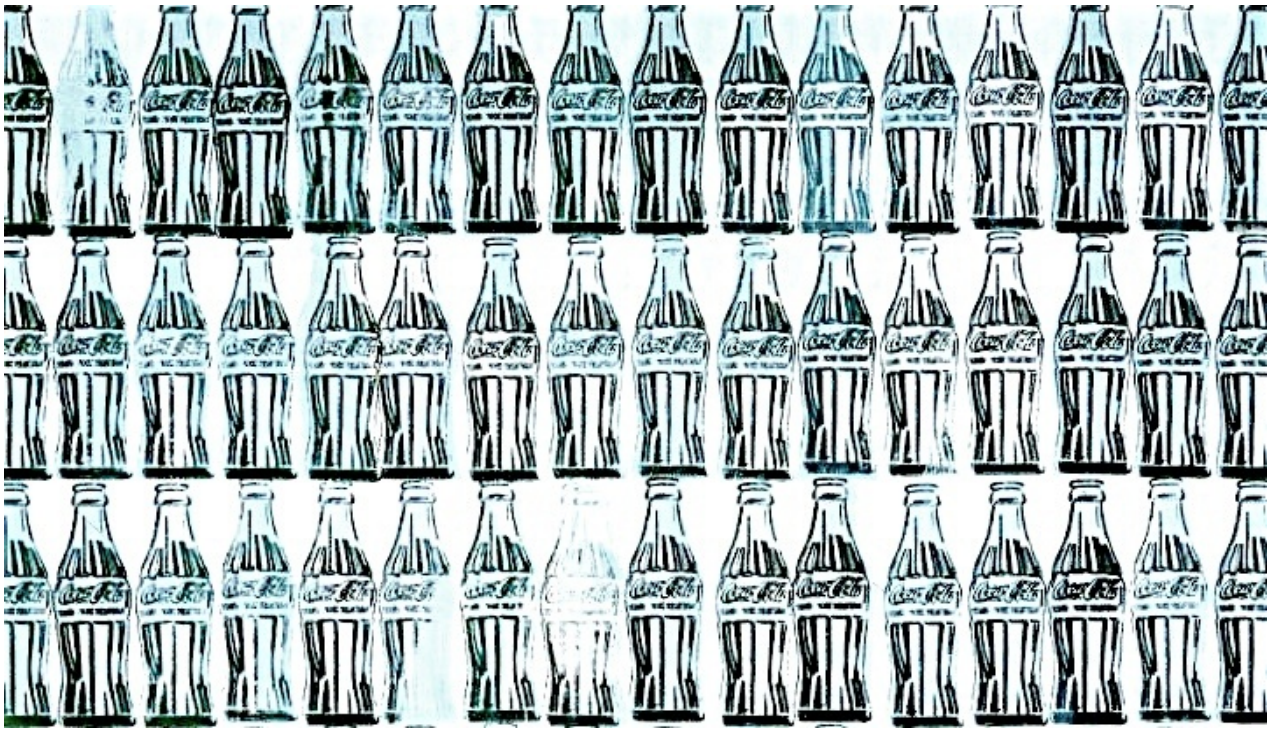

Green Coca-Cola Bottles (section), Andy Warhol, 1962

BL2: Periodicity

The essential feature that distinguishes the crystalline form as a state of matter is the existence, on the atomic scale, of some recurring structural unit — be it a single atom or a group of atoms — whose repeat extends at regular intervals in all three dimensions. The crystal is built up from from a tessellation of these identical units, much as a mosaic is assembled from a recurring motif of individual tiles. We refer to the repeating unit as a "unit cell". The contents of any one unit cell can be mapped directly onto the contents of another through translations alone.

Here is where the concept of convolution is so useful: it enables us to consider an entire crystal lattice as the contents of a single unit cell (what we call the "motif") *convoluted with* a lattice of points that describes the tessellation itself — how the unit cells are stacked together to form the crystal. In order to understand the Fourier transform of a crystal, all we need is to understand the Fourier transform of the motif and the Fourier transform of the lattice of points. We can take the product of these two transforms to arrive at the Fourier transform of the crystal itself.

In this lecture we will learn about lattices and their Fourier transforms. The first thing to clarify is that the lattice of points is just a mathematical object — there are no atoms or molecules involved, just points. As such, we need a concise mathematical way of representing a point, and the candidate here is a function known as the "Dirac delta function":

$$\delta(\mathbf{r}-\mathbf{r}_j) = \begin{cases} 0 & \mathbf{r} \neq \mathbf{r}_j \\ \infty & \mathbf{r} = \mathbf{r}_j \end{cases}, \tag{4}$$

$$\int \delta(\mathbf{r})\,\mathrm{d}\mathbf{r} = 1. \tag{5}$$

The first of these conditions stipulates that the function only has a non-zero value at a single position in space — namely, $\mathbf{r}_j$. The second condition normalises the function so that the integral across all space gives us a sum total of exactly one point. This means that when we form our convolution with the motif, we are placing precisely one copy of the motif at this point in space.

Let us see all this in action by considering a simple one-dimensional repeat: in this case, an SOS morse code signal:

To separate the motif from the lattice, we identify a recognisable part of the repeating signal, and note wherever this point recurs.

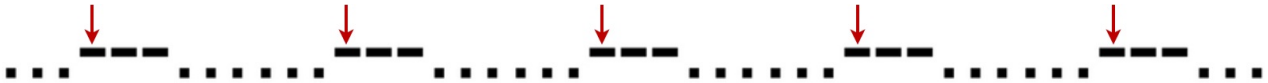

The locations of the arrows now give us the "lattice points", and the morse code between any two adjacent arrows is the motif. Note that we would obtain the same pattern of arrows — the same lattice — even if we chose a very different part of the signal as our reference point. Making use of our delta function terminology, we can represent the lattice itself as a series of delta functions, separated by some common distance a:

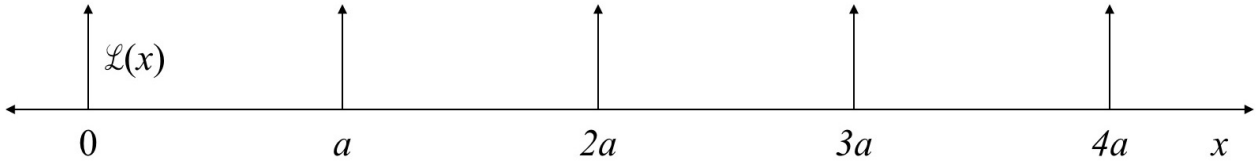

Mathematically, we write the lattice function $\mathcal{L}(x)$ as:

$$\mathcal{L}(x) = \sum_n \delta(x - na), \tag{6}$$

where n runs through all integers, positive and negative.

So the question now is to ask what the Fourier transform of this function looks like. We could do the mathematics (and indeed all is written out in gory detail in an appendix), and

calculate the Fourier transform $\mathcal{R}(Q) = \int \sum_n \delta(x - na) \exp(\mathrm{i}Qx)\,\mathrm{d}x$ directly. The result is a lattice itself, now running throughout reciprocal space:

$$\mathcal{R}(Q) = \sum_h \delta(Q - 2\pi h/a). \tag{7}$$

But it is perhaps more informative to visualise why this is the case — why is the Fourier transform of a lattice another lattice itself?

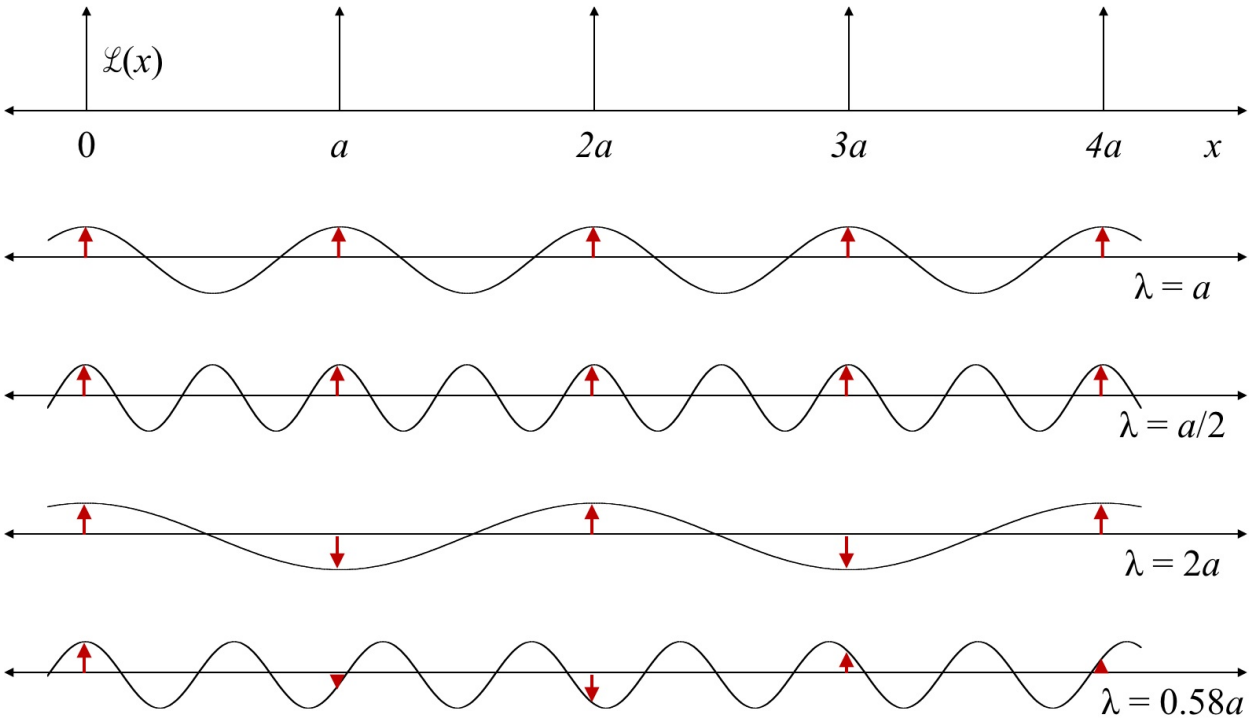

In evaluating the Fourier coefficient for a given wave, what we are really calculating is the extent to which the wave and the original function overlap. So, in the diagram above, we have drawn a number of different waves, chosen to illustrate which types give rise to non-zero Fourier coefficients, and which types have no net overlap with $\mathcal{L}(x)$. The first candidate is a wave whose wavelength matches the unit cell length a. $\mathcal{L}(x)$ is only non-zero at $x = na$, and so we only need worry about the height of the wave at each of these points. Because the wavelengths match exactly, there is the same positive overlap at each multiple of a, and we will end up with an infinitely large Fourier component for this wave. In fact, any wave whose wavelength is an integral fraction of a will give the same result: we see this in the case of $\lambda = a/2$, but it is clear that this will generalise to $\lambda = a/3, a/4, a/5, \ldots$. For all other cases, even if λ is an integral multiple of a, what happens is that there are as many positive contributions to the overlap as there are negative: the net overlap (the integral over all x) becomes zero.

Recall that we are defining periodicity in terms of a reciprocal space vector $\mathbf{Q}$, whose magnitude is related to the wavelength by $Q = 2\pi/\lambda$. So, the wave $\lambda = a$ corresponds to $Q = 2\pi/a$, $\lambda = a/2$ to $Q = 4\pi/a$, $\lambda = a/3$ to $Q = 6\pi/a$, and so on. So the Fourier

transform of $\mathcal{L}(x)$ is zero everwhere, except whenever $Q = 0, 2\pi/a, 4\pi/a, 6\pi/a, \ldots$, where it is infinite. This sounds very much like a series of evenly spaced delta functions, now situated in reciprocal space: precisely what equation (7) describes.

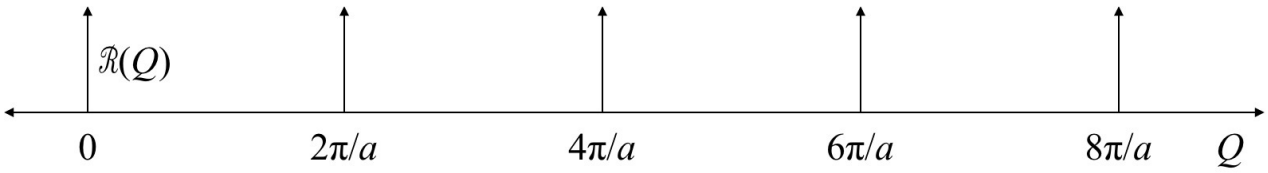

In real space, our lattice had a periodicity of a units. By contrast, the periodicity of the corresponding "reciprocal lattice" is $a^* = 2\pi/a$. If we increase the spacing in one, we decrease that in the other. Large unit cells in real space give rise to small reciprocal unit cells in reciprocal space; a large reciprocal unit cell implies a small real unit cell.

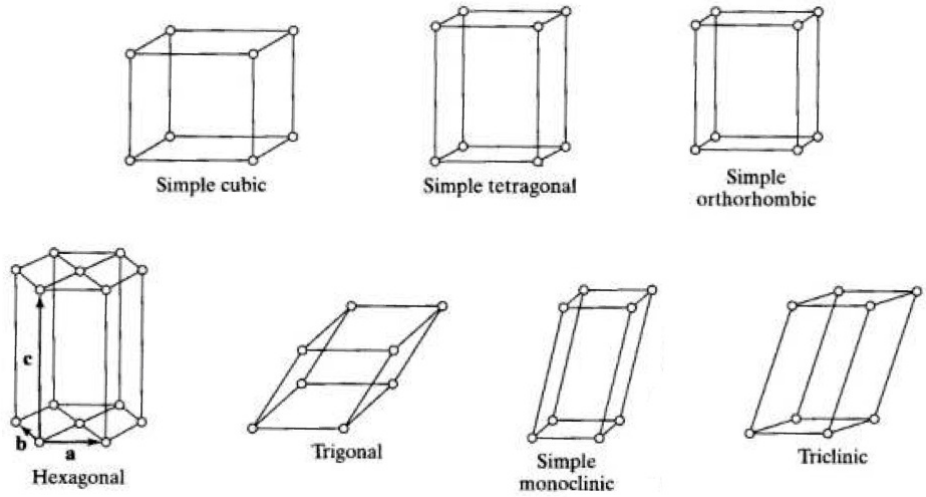

We need to extend these ideas to three dimensions, but first we will revise our understanding of crystal unit cells from last year. The key idea is that we can define any such cell in terms of three unit cell vectors, $\mathbf{a}$, $\mathbf{b}$ and $\mathbf{c}$, giving the "lattice parameters" a, b and c (the lengths of the unit cell vectors), and α, β and γ (the angles between $\mathbf{b}$ and $\mathbf{c}$, $\mathbf{c}$ and $\mathbf{a}$, and $\mathbf{a}$ and $\mathbf{b}$, respectively). Depending on the relationships between these various parameters, we assign the lattice to one of 7 different classes:

Class	**Conditions**	
Cubic	$a = b = c$,	$\alpha = \beta = \gamma = 90°$
Tetragonal	$a = b \neq c$,	$\alpha = \beta = \gamma = 90°$
Orthorhombic	$a \neq b \neq c$,	$\alpha = \beta = \gamma = 90°$
Hexagonal	$a = b \neq c$,	$\alpha = \beta = 90°$, $\gamma = 120°$
Trigonal (Rhombohedral)	$a = b = c$,	$\alpha = \beta = \gamma \neq 90°$
Monoclinic	$a \neq b \neq c$,	$\alpha = \gamma = 90°$, $\beta \neq 90°$
Triclinic	$a \neq b \neq c$,	$\alpha \neq \beta \neq \gamma \neq 90°$

In our new language of delta functions, we describe these three-dimensional lattices in terms of a function $\mathcal{L}(\mathbf{r})$:

$$\mathcal{L}(\mathbf{r}) = \sum_{UVW} \delta[\mathbf{r} - (U\mathbf{a} + V\mathbf{b} + W\mathbf{c})]. \tag{8}$$

Then the Fourier transform of this lattice is, as for the one-dimensional case, another lattice:

$$\mathcal{R}(\mathbf{Q}) = \sum_{hkl} \delta[\mathbf{Q} - (h\mathbf{a}^* + k\mathbf{b}^* + l\mathbf{c}^*)]. \tag{9}$$

The "reciprocal lattice vectors" $\mathbf{a}^*$, $\mathbf{b}^*$ and $\mathbf{c}^*$ generate the reciprocal space lattice, and they are given by the equations:

$$\mathbf{a}^* = 2\pi \frac{\mathbf{b} \times \mathbf{c}}{\mathbf{a} \cdot (\mathbf{b} \times \mathbf{c})}, \qquad \mathbf{b}^* = 2\pi \frac{\mathbf{c} \times \mathbf{a}}{\mathbf{b} \cdot (\mathbf{c} \times \mathbf{a})}, \qquad \mathbf{c}^* = 2\pi \frac{\mathbf{a} \times \mathbf{b}}{\mathbf{c} \cdot (\mathbf{a} \times \mathbf{b})}. \tag{10}$$

These equations look more complicated than they actually are. Their derivation is given as an appendix, but we are really only concerned with their meaning (the important thing, after all). In each case, the cross product contained in the numerator produces a vector that is perpendicular to the two real-space axes involved. That is, $\mathbf{b} \times \mathbf{c}$ — and hence $\mathbf{a}^*$ — is perpendicular to $\mathbf{b}$ and $\mathbf{c}$. In cases where $\mathbf{a}$, $\mathbf{b}$ and $\mathbf{c}$ are not orthogonal (such as in hexagonal systems), then $\mathbf{a}^*$ may not necessarily be parallel to $\mathbf{a}$, and so on. The denominator is actually the same value in each case: namely, the unit cell volume. It scales the vector to the correct length, and it's not too hard to see that in simple systems we end up with what we expect based on the one-dimensional example.

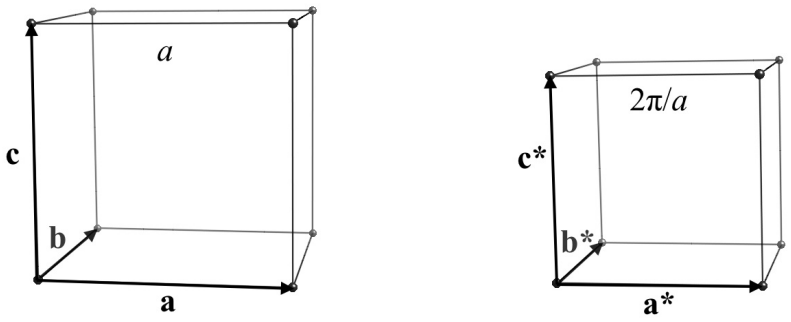

Let us consider the case of a simple cubic lattice, illustrated above. The solid points in this picture correspond to three-dimensional delta functions $\delta(\mathbf{r})$, and the unit cell vectors are aligned with cartesian axes $\mathbf{i}, \mathbf{j}, \mathbf{k}$ such that $\mathbf{a} = a\mathbf{i}$, $\mathbf{b} = a\mathbf{j}$ and $\mathbf{c} = a\mathbf{k}$. In evaluating the reciprocal lattice, we find (*e.g.*) $\mathbf{b} \times \mathbf{c} = a^2\mathbf{i}$, and that $\mathbf{a} \cdot (\mathbf{b} \times \mathbf{c}) = a^3$. Substituting these values into the equation for $\mathbf{a}^*$ given in (10), one obtains $\mathbf{a}^* = \frac{2\pi}{a}\mathbf{i}$. Similarly, $\mathbf{b}^* = \frac{2\pi}{a}\mathbf{j}$ and $\mathbf{c}^* = \frac{2\pi}{a}\mathbf{k}$. So, the reciprocal lattice is also a cubic lattice, but now with a edge length of

$2\pi/a$. The inverse relationships we noted for the one dimensional case apply here too: the larger the real space unit cell, the smaller the reciprocal space unit cell.

We can already say something about the Fourier transform we expect for a crystal with this simple cubic symmetry. *Irrespective* of the chemical composition, or the arrangement of atoms within the unit cell, we know that the Fourier transform will be the product of the transform of the motif and the that of the cubic lattice. We now know that the latter is itself a cubic lattice — zero nearly everywhere in reciprocal space, except at each of the reciprocal lattice points. So the total product must also be zero nearly everywhere: it too will look like a lattice, except that the values at each of the lattice points will be determined by the Fourier transform of the motif at the same points in reciprocal space. Writing this in terms of equation (1), we have:

$$F_{\text{crystal}}(\mathbf{Q}) = F_{\text{unitcell}}(\mathbf{Q}) \times \mathcal{R}(\mathbf{Q}) \tag{11}$$

$$= \int_{\text{unitcell}} \rho(\mathbf{r}) \exp(\mathrm{i}\mathbf{Q}\cdot\mathbf{r})\,\mathrm{d}\mathbf{r} \times \sum_{hkl} \delta[\mathbf{Q} - (h\mathbf{a}^* + k\mathbf{b}^* + l\mathbf{c}^*)], \tag{12}$$

which is only non-zero for $\mathbf{Q} = h\mathbf{a}^* + k\mathbf{b}^* + l\mathbf{c}^*$. Expanding each point $\mathbf{r}$ in terms of its components x, y, z along the real-space unit cell vectors, we have:

$$F_{\text{crystal}}(hkl) = \int_{\text{unitcell}} \rho(\mathbf{r}) \exp[\mathrm{i}(h\mathbf{a}^* + k\mathbf{b}^* + l\mathbf{c}^*)\cdot(x\mathbf{a} + y\mathbf{b} + z\mathbf{c})]\,\mathrm{d}\mathbf{r} \tag{13}$$

$$= \int_{\text{unitcell}} \rho(\mathbf{r}) \exp[2\pi\mathrm{i}(hx + ky + lz)]\,\mathrm{d}\mathbf{r}. \tag{14}$$

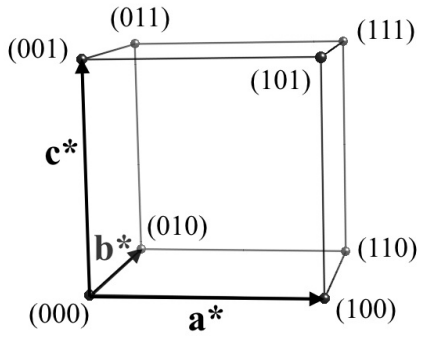

We finish this lecture by commenting that it is customary to label reciprocal lattice points by the corresponding values h, k, l, using the notation (hkl) as in the figure above. We met this notation last year in IA, where we used it to designate peaks in a diffraction pattern (and the corresponding planes in real space). Our aim in the next lecture, BL3, is to see how these two concepts — diffraction from "planes" of atoms and the reciprocal lattice — are intimately related.

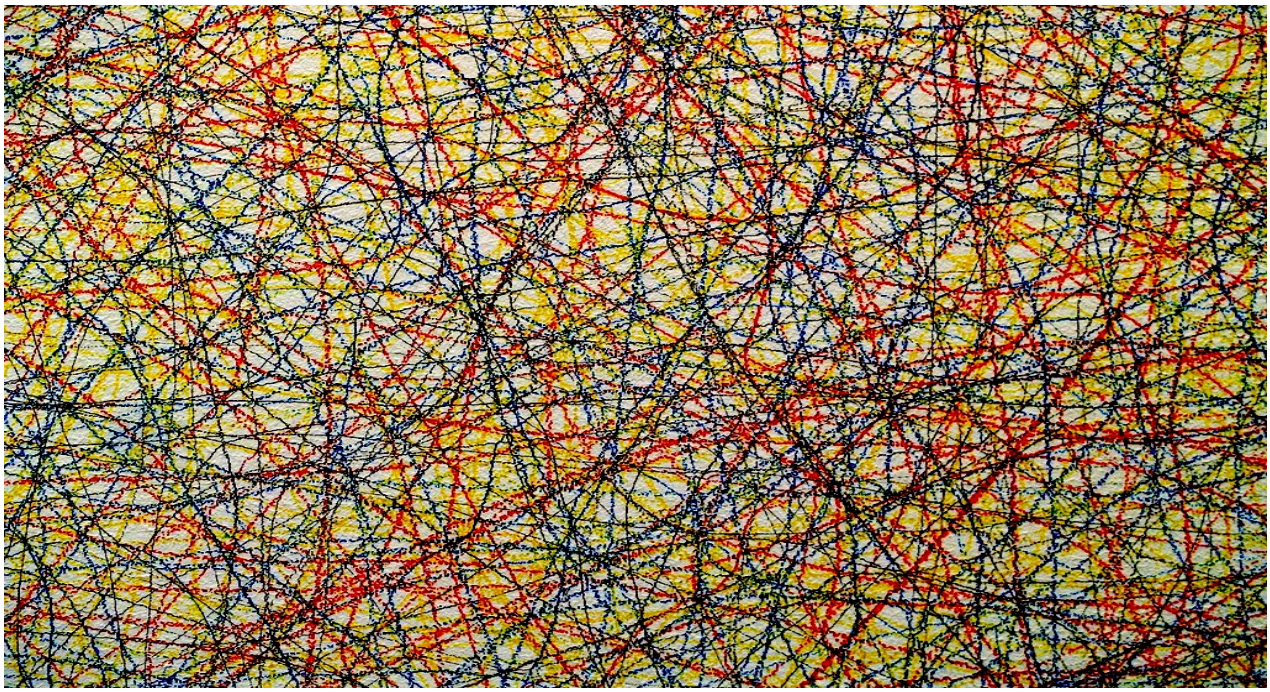

Wall Drawing #65, Sol Lewitt, 1971

BL3: Diffraction Geometry

We have now seen, in the first two lectures, how material structure can be thought of in terms of reciprocal space — a bizarre world where the arrangement of atoms is built up from a superposition of different waves. Reciprocal space is actually quite a central concept in much of solid state chemistry and condensed matter physics, so it is a concept worth understanding in itself. But its particular relevance in a mineral sciences context is that it is a reciprocal-space view of material structure that one obtains in a diffraction experiment. When we shine a suitable beam of radiation at a crystal, the beam diffracts, and the pattern of spots we see is actually a direct view of the reciprocal lattice we learned about in BL2. Our goal in this lecture is to explain how this diffraction process works, and to show how the reciprocal space formalisms we have already developed are consistent with the Bragg equations we studied in IA Materials and Minerals.

The diffraction process begins with a beam of radiation, which we consider to be a wave propagating through space. The types of radiation usually used are x-rays or neutrons,

and we will cover these in greater depth in BL4. For the time being, the important concept is that this radiation is a wave and, as such, can be described by a wave-vector $\mathbf{k}_\mathrm{i}$ ("i" here to signify "incident"), much in the same way that we used $\mathbf{Q}$ to describe waves in previous lectures. Specifically, the vector $\mathbf{k}_\mathrm{i}$ is parallel to the direction of propagation of the incident beam and its magnitude is inversely proportional to the wavelength: $k_\mathrm{i} = |\mathbf{k}_\mathrm{i}| = 2\pi/\lambda$. After interacting with the crystal, the beam is diffracted such that it now propagates along a different direction, and we denote this scattered wave by $\mathbf{k}_\mathrm{s}$. For elastic scattering — the only type of scattering we will worry about in this lecture course — there is no transfer of energy from the beam of radiation to the sample. So the wavelengths of the incident and scattered beams (a direct measure of their energy) are equal; all that changes is the direction of the wave-vector. We can write trivial equations for the incident and scattered beams:

$$\psi_\mathrm{i}(\mathbf{x}) = A\exp(\mathrm{i}\mathbf{k}_\mathrm{i}\cdot\mathbf{x}), \quad (15)$$

$$\psi_\mathrm{s}(\mathbf{x}) = A\exp(\mathrm{i}\mathbf{k}_\mathrm{s}\cdot\mathbf{x}), \quad (16)$$

where A is some arbitrary amplitude of the waves.

It is the scattered waves from a very large number of such events that add up to give the diffraction pattern we observe. Some interfere constructively with one another such that at appropriate points one records a heavily amplified signal. At other points the waves have essentially cancelled one another.

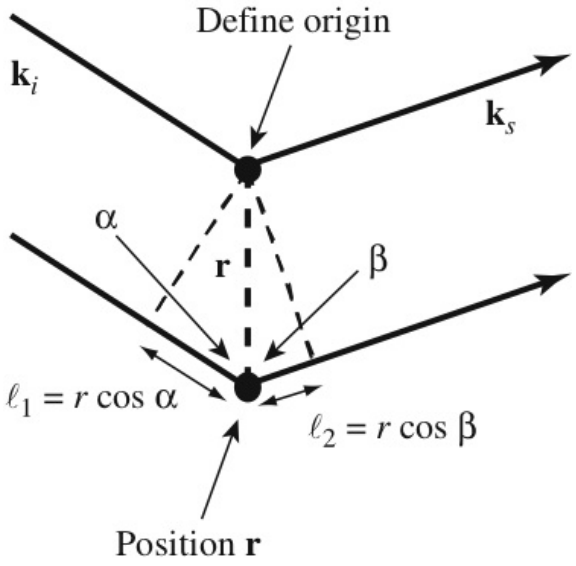

Let us quantify this interference more precisely by considering the situation illustrated above. Here a beam of radiation with initial wave-vector $\mathbf{k}_\mathrm{i}$ is scattered by a pair of identical particles, separated from one another by the vector $\mathbf{r}$. The key point is that the two scattering processes — which, locally, are equivalent — in fact involve slightly different path lengths. The ray that scatters from the atom at position $\mathbf{r}$ in the diagram has travelled further than that scattered from the atom at the origin.

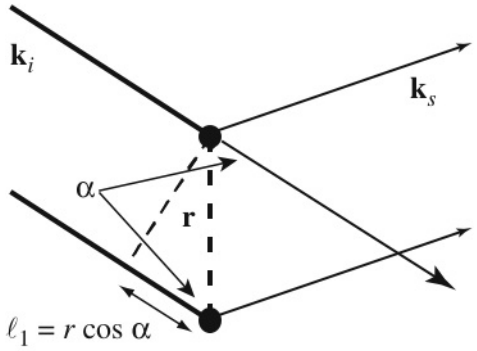

We can calculate this difference in path lengths using simple trigonometry. First, we divide the additional distance concerned into two separate segments: these are labelled ℓ_1 and ℓ_2 in the diagram. The lengths of these two segments can be expressed in terms of the interatomic separation $r = |\mathbf{r}|$ and the angles α and β, formed by the vector $\mathbf{r}$ with the incident and scattered rays, respectively. Considering ℓ_1 first, we start by writing $\cos\alpha$ in terms of the vectors $\mathbf{k}_\mathrm{i}$ and $\mathbf{r}$:

$$\mathbf{k}_\mathrm{i} \cdot \mathbf{r} = k_\mathrm{i} \times r \times \cos\alpha = \frac{2\pi}{\lambda} r \cos\alpha. \tag{17}$$

Substituting $\ell_1 = r\cos\alpha$ into this expression, we obtain

$$\ell_1 = \frac{\lambda}{2\pi} \mathbf{k}_\mathrm{i} \cdot \mathbf{r}. \tag{18}$$

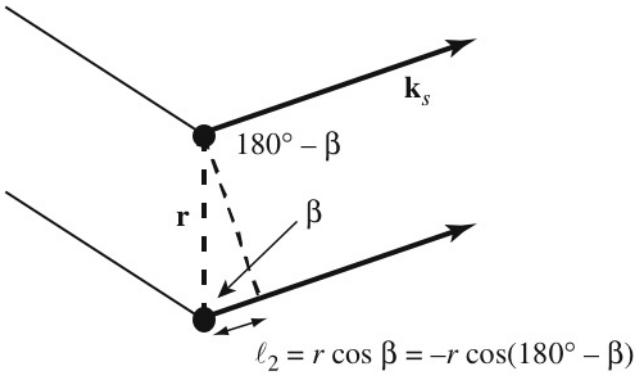

We apply the same approach now to evaluating ℓ_2, first by writing $\cos\beta$ in terms of $\mathbf{k}_\mathrm{s}$ and $\mathbf{r}$:

$$\mathbf{k}_\mathrm{s} \cdot \mathbf{r} = k_\mathrm{s} \times r \times \cos(\pi - \beta) = -\frac{2\pi}{\lambda} r \cos\beta. \tag{19}$$

Finally, we substitute $\ell_2 = r\cos\beta$ into this expression to give

$$\ell_2 = -\frac{\lambda}{2\pi} \mathbf{k}_\mathrm{s} \cdot \mathbf{r}. \tag{20}$$

So, the total additional path length $\ell_1 + \ell_2$ is $\frac{2\pi}{\lambda}(\mathbf{k}_\mathrm{i} - \mathbf{k}_\mathrm{s}) \cdot \mathbf{r}$, which is equivalent to a phase shift of $(\mathbf{k}_\mathrm{i} - \mathbf{k}_\mathrm{s}) \cdot \mathbf{r}$ between the two scattered waves. What this means is that if the wave scattered from the particle at the origin is given by the equation $\psi_1(\mathbf{x}) = A\exp(\mathrm{i}\mathbf{k}_\mathrm{s} \cdot \mathbf{x})$, that scattered by the atom at position $\mathbf{r}$ will be $\psi_2(\mathbf{x}) = A\exp(\mathrm{i}\mathbf{k}_\mathrm{s} \cdot \mathbf{x}) \times \exp[\mathrm{i}(\mathbf{k}_\mathrm{i} - \mathbf{k}_\mathrm{s}) \cdot \mathbf{r}]$. The interference pattern — the sum of the two waves — is then given by

$$\psi_1(\mathbf{x}) + \psi_2(\mathbf{x}) = A\exp(\mathrm{i}\mathbf{k}_\mathrm{s} \cdot \mathbf{x}) \times \{1 + \exp[\mathrm{i}(\mathbf{k}_\mathrm{i} - \mathbf{k}_\mathrm{s}) \cdot \mathbf{r}]\}. \tag{21}$$

One interesting property highlighted by this equation is that the interference pattern is not sensitive to the actual wave-vectors $\mathbf{k}_\mathrm{i}$ and $\mathbf{k}_\mathrm{s}$, but only to their difference. Because of this, we can formulate our scattering equations in terms of a single wave-vector $\mathbf{Q} = \mathbf{k}_\mathrm{i} - \mathbf{k}_\mathrm{s}$. This is precisely the same $\mathbf{Q}$ we have already met in BL1 and BL2. Rewriting equation (21) in this light, we can say that the scattered beam has been modified by a factor

$$F(\mathbf{Q}) = 1 + \exp(\mathrm{i}\mathbf{Q} \cdot \mathbf{r}) = \exp(\mathrm{i}\mathbf{Q} \cdot \mathbf{0}) + \exp(\mathrm{i}\mathbf{Q} \cdot \mathbf{r}). \tag{22}$$

It is straightforward to extend this idea to a collection of arbitrarily many point particles at positions $\mathbf{r}_1$, $\mathbf{r}_2$, $\mathbf{r}_3, \ldots$ to give the general "scattering factor":

$$\begin{aligned} F(\mathbf{Q}) &= \exp(\mathrm{i}\mathbf{Q} \cdot \mathbf{r}_1) + \exp(\mathrm{i}\mathbf{Q} \cdot \mathbf{r}_2) + \exp(\mathrm{i}\mathbf{Q} \cdot \mathbf{r}_3) + \ldots & (23)\\ &= \sum_j \exp(\mathrm{i}\mathbf{Q} \cdot \mathbf{r}_j). & (24)\end{aligned}$$

Indeed, by converting this sum to an integral over all space we allow a further generalisation to arbitrary particle distributions (*i.e.* allowing for non-point particles):

$$F(\mathbf{Q}) = \int \rho(\mathbf{r}) \exp(\mathrm{i}\mathbf{Q} \cdot \mathbf{r})\, \mathrm{d}\mathbf{r}. \tag{25}$$

This equation should be entirely familiar. What we have shown here is quite remarkable: namely, that the scattering process is nothing but a Fourier transformation itself. In a diffraction experiment, the scattered wave characterised by $\mathbf{k}_\mathrm{s}$ tells us about the Fourier component at the wave-vector $\mathbf{Q} = \mathbf{k}_\mathrm{i} - \mathbf{k}_\mathrm{s}$. By measuring the scattered waves for different wave-vectors $\mathbf{k}_\mathrm{s}$ (and, effectively, for different $\mathbf{Q}$), we can actually piece together a picture of reciprocal space. Diffraction is an experimental technique that allows us to view reciprocal space directly.

Well, almost. There is (as always) one fundamental problem. Namely, that when we detect a scattered wave such as $F(\mathbf{Q})$, what we are measuring is not the wave itself, but some intensity $I(\mathbf{Q})$ that is proportional to the square of its modulus: $I(\mathbf{Q}) \propto |F(\mathbf{Q})|^2$. This intensity is a real positive value, whereas the amplitude $F(\mathbf{Q})$ is a complex number. By measuring intensity rather than amplitude we have surrendered all information about the phase of the amplitude. In terms of our cat/duck Fourier transform illustrations of BL1, what

we are saying is that we measure the intensity of the colours in the Fourier images, but not the colours themselves. This makes it very difficult to reconstruct a real-space description of structure from what is an incomplete "colour-blind" reciprocal-space description. Known as the "phase problem", this issue forms the subject of the final lecture in our course, BL9. One very important help in solving this problem is an understanding of symmetry in crystalline materials. We will spend some time learning about symmetry and its effect on diffraction patterns — the subject of lectures BL5 through to BL8.

For the time being, we will concern ourselves a little more with the geometry of diffraction experiments, and the relationship between the various quantities involved. The first thing we will do is to relate our scattering vector $\mathbf{Q}$ to the various diffraction concepts we first encountered in IA: namely, the Bragg diffraction angle 2θ, d-spacing and the Bragg law. Reminding ourselves of the scattering geometry illustrated in the diagram on page BH 15, we begin with the relationship

$$\begin{aligned} Q^2 = |\mathbf{Q}|^2 &= |\mathbf{k}_\mathrm{i} - \mathbf{k}_\mathrm{s}|^2 = k_i^2 + k_s^2 && (26)\\ &= k_\mathrm{i}^2 + k_\mathrm{s}^2 - 2k_\mathrm{i}k_\mathrm{s}\cos 2\theta && (27)\\ &= 2\left(\frac{2\pi}{\lambda}\right)^2 - 2\left(\frac{2\pi}{\lambda}\right)^2 \cos 2\theta && (28)\\ &= \frac{16\pi^2}{\lambda^2}\sin^2\theta, && (29) \end{aligned}$$

where we have used the identity $1 - \cos 2\theta = 2\sin^2\theta$. Consequently, the magnitude Q of the scattering vector is related to the Bragg angle θ by the equation

$$Q = \frac{4\pi}{\lambda}\sin\theta. \qquad (30)$$

Note that because the experimental limit of θ is 90° (*i.e.* $2\theta_\mathrm{max} = 180^\circ$) then there is a maximum measurable value of Q: namely, $Q_\mathrm{max} = 4\pi/\lambda$.

Bragg's law told us that we expect to see a diffraction peak corresponding to the Bragg angle θ whenever there were a set of atomic planes separated by the distance $d = \lambda/2\sin\theta$. Recasting this in terms of Q, we have

$$Q = \frac{2\pi}{d}. \qquad (31)$$

Hopefully this should make complete sense in terms of our picture of the reciprocal lattice. We now know, from BL2, that we expect only to see components in reciprocal space whenever $\mathbf{Q}$ is a reciprocal lattice vector $\mathbf{Q} = h\mathbf{a}^* + k\mathbf{b}^* + l\mathbf{c}^*$. The corresponding magnitude of Q is quite easy to calculate in the case where the lattice (and reciprocal lattice) is orthogonal: by Pythagoras we have

$$Q = \left[(ha^*)^2 + (kb^*)^2 + (lc^*)^2\right]^{1/2} \tag{32}$$

$$= \left[\frac{4\pi^2h^2}{a^2} + \frac{4\pi^2k^2}{b^2} + \frac{4\pi^2l^2}{c^2}\right]^{1/2}, \tag{33}$$

which, when substituted into equation (31) gives us the (hopefully) familiar expression for d-spacing in an orthogonal crystal:

$$\frac{1}{d^2} = \frac{h^2}{a^2} + \frac{k^2}{b^2} + \frac{l^2}{c^2}. \tag{34}$$

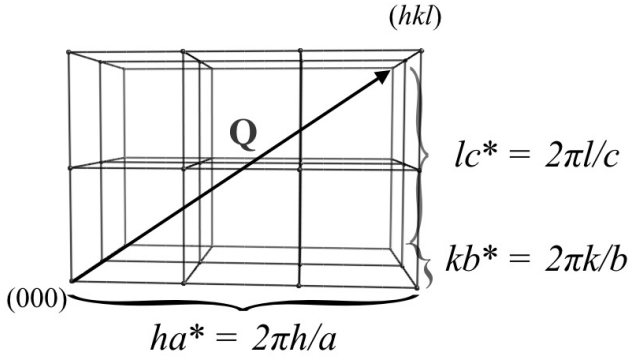

We will conclude with two comments about the relationship between 2θ and Q.

(i) If the scattered and incident beams are parallel, we have $2\theta = 0$ and hence $Q = 0$. We can think of this as corresponding to the (000) point in reciprocal space. Note that at this value of $\mathbf{Q}$, equation (25) reduces to $F(\mathbf{0}) = \int \rho(\mathbf{r})\,\mathrm{d}\mathbf{r}$ — the total amount of material.

(ii) There is a physical limitation on the maximum value of 2θ that one can measure: namely, $2\theta = 180°$. This means that we can only measure reciprocal space up to a maximum value $Q_{\max} = 4\pi/\lambda$ (by equation (30)). The use of shorter wavelengths λ would enable us to measure more of reciprocal space, but we will never be able to measure everything.

So, in summary, we have shown that diffraction is an experimental technique that allows us to visualise the Fourier transform of a crystal. It gives us a means of observing the reciprocal lattice itself, from which we will hope to recover information about the distribution of atomic density in the crystal sample. We know that this is going to be difficult, because we lose phase information about the Fourier transform. Also, we are limited in that we can never observe all of reciprocal space — only a region up to some value $Q_{\max}$, determined by the wavelength of the radiation used. In the next lecture, BL4, we discuss the different types of radiation typically used, and also the actual experimental approach taken to measuring diffraction patterns.

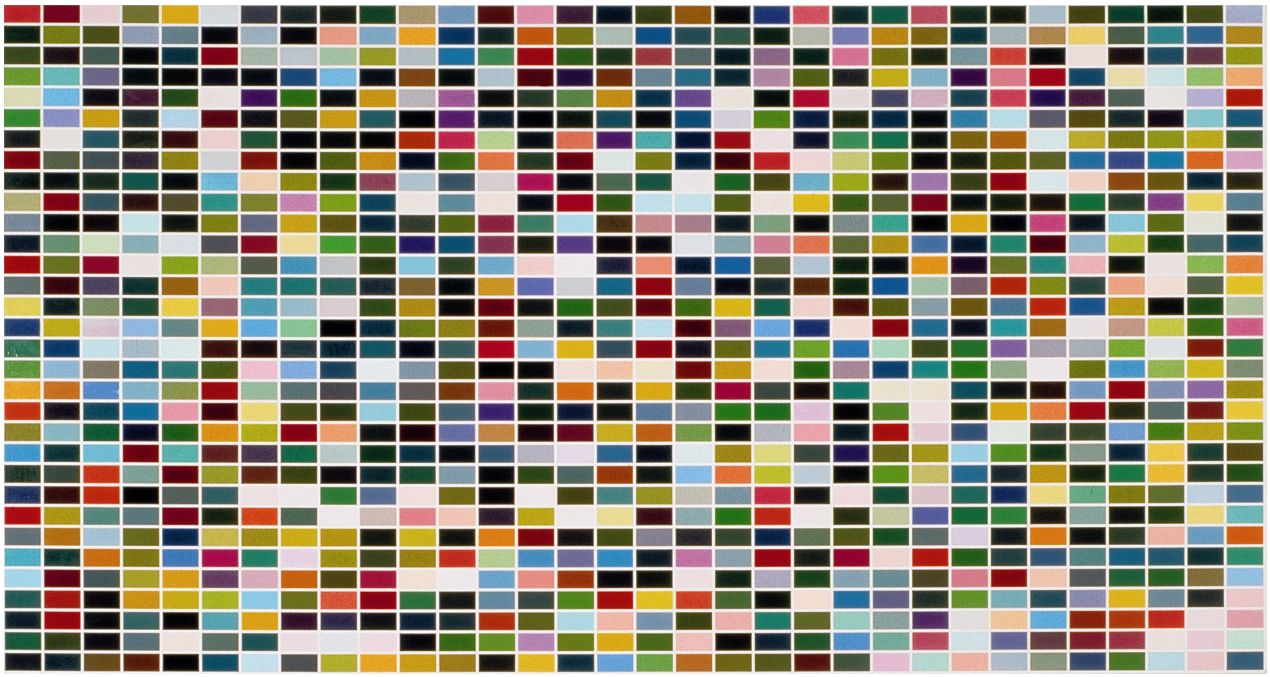

1024 Farben, Gerhard Richter, 1973

BL4: Experimental Techniques

We saw in BL3 that the amount of reciprocal space one can measure in a diffraction experiment is limited by the wavelength of the radiation used: $Q_{\max} = 4\pi/\lambda$, where the Fourier components have a wavelength of $2\pi/Q_{\max} = \lambda/2$. The physical meaning of this minimum wavelength is that it corresponds to the finest level of detail in real space that one can hope to resolve from a reverse Fourier transform of the diffraction data. We have already seen that the exclusion of high frequency components in our Fourier duck (page BH 7) meant that we could not distinguish either its beak or its wings. So, if we are to distinguish neighbouring atoms from one another, we will need a sufficiently small wavelength to give a real-space resolution of about 1 Å.

There are two principal types of radiation that satisfy this requirement. The first is a beam of x-rays, and the second is a beam of thermal neutrons. There are many similarities between these two sources of radiation — certainly they both produce diffraction patterns as described in lecture BL3. But there are a number of important differences, due primarily to the different physics associated with their scattering mechanisms. In this lecture, we will discuss the two types of diffraction techniques, highlighting the strengths and weaknesses of each method. The overall message is that we can obtain complementary information from x-ray diffraction and neutron diffraction: much of the cutting-edge science in the field exploits features of both techniques.

X-rays are the part of the electromagnetic spectrum with wavelengths in the range 0.1–100 Å, and hence with energies in the range 10^2–10^5 eV. To appreciate this energy scale,

we note that the kinetic energy of an atom in a gas at room temperature is 0.025 eV. Indeed, x-rays are sufficiently energetic to ionise atoms, and can interfere with the chemistry of materials over even quite short periods.

In the laboratory, x-rays are produced when a beam of electrons strikes a metal target. The x-rays are actually produced in two ways. First, the electrons are rapidly decelerated when they enter the metal, and an accelerating or decelerating charge will automatically produce electromagnetic radiation. This mechanism gives rise to a broad distribution of x-ray energies commensurate with the energies of the incident electrons. The second (and typically more useful) mechanism of x-ray production occurs when an electron strikes one of the metal atoms and causes an inner-shell electron to be ejected. An outer shell electron then relaxes into the now-partially-vacant inner shell, and emits an x-ray photon of a characteristic energy. For us, the important case is that of electrons falling from the L to the K shells (*i.e.* from the second to the first shell), and this transition is labelled $K\alpha$. This transition will have different energies (and hence produce x-rays of different wavelengths) for different metal targets:

Transition	**Wavelength (Å)**	**Transition**	**Wavelength (Å)**
Ti$K\alpha_1$	2.47851	Cr$K\alpha_1$	2.28962
Fe$K\alpha_1$	1.93597	Co$K\alpha_1$	1.78896
Cu$K\alpha$	1.54184	Mo$K\alpha$	0.711445
Ag$K\alpha$	0.561603	Ta$K\alpha_1$	0.215947
W$K\alpha_2$	0.20901	Au$K\alpha_1$	0.180195

The traditional method of recording and measuring x-ray diffraction patterns is to use photographic film that has been optimised for x-rays. This is ideal for obtaining a wide sweep of the diffraction pattern in one measurement. The "greyness" of each reflection can be measured by optical methods and converted into a relative intensity. Several diffraction photographs may be required in order to record the range from very strong to very weak, since the strong reflections can easily saturate the film. The alternative method of measuring x-ray intensities is to use a detector (or "counter"). This has the advantage over films of giving the intensity directly and more accurately. The disadvantage is that a single detector will only record a single point in reciprocal space at any one time. This problem can be overcome by using area detectors that contain a large number of pixels, each of which is capable of recording its own signal. These are now the most widely used form of detector.

One fundamental limitation on the use of x-ray tubes is that the maximum intensity is limited by the need to prevent overheating of the target. X-ray production is not very efficient, and most of the energy of the incident electron beam is lost as heat. This can be overcome in part by using rotating targets, so that the electron beam does not strike a single area of the target. However, there is still a mechanical limitation on the maximum intensity produced. Moreover, the wavelength of x-rays produced by a given x-ray tube is determined by the nature of its metal target, and so is not variable.

Synchrotron sources provide a mechanism of circumventing these limitations. A synchrotron is a very large experimental facility that uses a ring of magnets of some tens of metres in radius to accelerate a beam of electrons in a circular orbit. An electron travelling in a circular orbit is constantly accelerating in a radial direction and decelerating in the direction of the tangent. Thus the circular beam continuously loses energy as photons: this process is called "synchrotron radiation". This radiation is in fact a nuisance for particle physicists, but for the generation of an intense beam of high-energy photons it is ideal. The quality of the beam can be enhanced further by the use of devices that give a special "kick" to the electrons at regular intervals. The ESRF synchrotron facility at Grenoble is shown in the picture above. The large ring in the foreground contains the circular path around with the electrons are accelerated.

There are two clear advantages of synchrotron radiation over standard x-ray tubes.

(i) The wavelength is completely tuneable: it can be selected from a broad distribution by Bragg reflection from a monochromator crystal. This is important in special types of diffraction experiments where one aims to choose an x-ray photon energy close to a resonant absorption energy of one of the atoms in the crystal being studied.

(ii) The intensity is increased by many orders of magnitude. This permits the use of smaller crystals, increases the resolution of the observed diffraction patterns and allows incredibly fast measurements so that kinetic studies can be performed.

The second type of radiation, namely a beam of thermal neutrons, can be produced in one of two ways. The "traditional" method is to generate beams of neutrons within a nuclear reactor. These are produced in the form of a broad spectrum. Individual wavelengths can be selected by Bragg diffraction from a crystal monochromator (as for x-rays). In this situation the diffraction equipment that utilises the neutron beam is similar in principle to that used with laboratory x-ray beams. The primary difference is one of scale: the neutron apparatus is typically much larger. In addition to scale, there is a key environmental problem in this method of producing neutrons, perhaps unsurprisingly, requires a nuclear reactor

A modern alternative source of neutrons — the second method of generating thermal neutrons alluded to above — is called a "spallation source". At such a facility, the production of neutrons begins when a beam of high-energy protons is fired into a heavy-metal target (such as tungsten). The protons strike the nuclei and eject high-energy neutrons. In fact the energies of these neutrons are too high to be useful, so they are slowed down by a moderating material (*e.g.* liquid methane). The moderator acts to absorb much of the neutrons' energy, producing a spectrum of neutrons with useable wavelengths. Different moderators produce slightly different distributions of wavelengths, and this property can be exploited for various applications.

The initial beam of protons is pulsed, so the beam of neutrons is also produced in a series of discrete pulses. The neutron scattering instrumentation at a spallation source exploits the pulsed nature of the neutron beam by measuring the wavelength by time-of-flight techniques. This avoids the wastage incurred by selecting individual wavelengths with a monochromator. Perhaps the world's leading neutron spallation source is a UK facility called ISIS; a view from inside the experimental hall is shown in the picture above. The slightly curved casing just to the left of centre in this picture contains the target where the thermal neutrons are produced.

A neutron diffraction experiment is more complicated and expensive than an x-ray diffraction experiment. Indeed, for the vast majority of routine applications x-ray diffraction is unquestionably the preferred method. There are, however, five key reasons why neutron scattering methods are useful:

(i) The hydrogen atom is virtually invisible to x-rays but will scatter neutrons with the same order of strength as any other atom. For crystallographic problems where the positions of hydrogen atoms are important (*e.g.* where there are C–H and O–H bonds), neutron scattering is the main way of providing information about the bond lengths.

(ii) In structures where there is an atom that dominates most of the x-ray scattering (typically atoms with a large number of electrons), the positions of other, lighter atoms (such as oxygen) may be difficult to deduce accurately. In neutron scattering, the scattering power of most atoms are broadly in the same range, so there is rarely a problem with one atom dominating the scattering.

(iii) We will show below that with x-rays the scattering power of each atom is proportional to the number of electrons, whereas with neutrons there is no correlation between the atomic number and the scattering power of an atom. Thus neutrons may be better at distinguishing between atoms that have a similar number of electrons, such as the Si^{4+} and Al^{3+} cations.

(iv) We will also see that with x-rays the scattering power of an atom falls off with increasing Q, whereas with neutrons the scattering power is independent of the scattering angle. For studies where we need scattering at high angles — *e.g.* to obtain accurate bond lengths in disordered systems — neutron scattering may be the preferred method.

(v) Neutrons have a magnetic moment, and so are sensitive to magnetic moments in crystals. As a consequence, neutron diffraction can give information about magnetic structure in magnetic materials.

How do we explain these differences between x-ray diffraction and neutron diffraction? The key is that the scattering process in x-ray diffraction occurs via interaction of the x-rays with the electron cloud of each atom in the material; whereas in neutron diffraction the interaction is with the atomic nuclei. So, while the wavelengths used in each type of experiment are usually very similar, the interactions occur over vastly different length scales. To see why this makes a difference, let us consider the scattering of x-rays by a single atom. If we denote the electron density by $\rho_{\rm el}(\mathbf{r})$, the scattering function will be

$$f(\mathbf{Q}) = \int_{\rm atom} \rho_{\rm el}(\mathbf{r}) \exp(\mathrm{i}\mathbf{Q}\cdot\mathbf{r})\,\mathrm{d}\mathbf{r}. \tag{35}$$

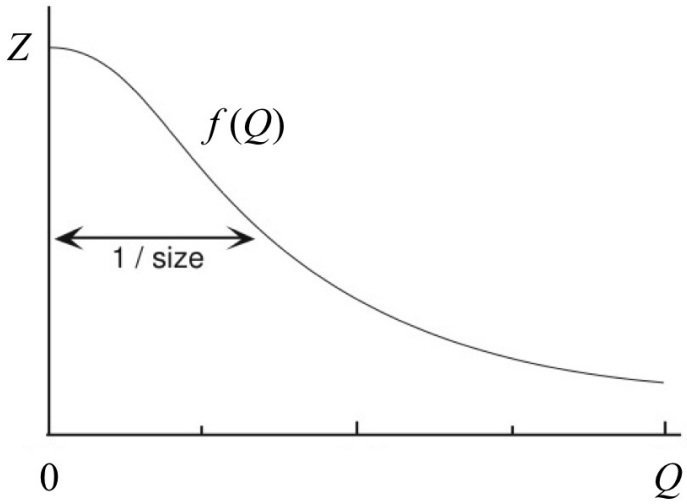

In the limit $Q \to 0$ we have $f(0) = \int \rho(\mathbf{r})\,\mathrm{d}\mathbf{r} = Z$, the number of electrons in the atom or ion. But it turns out that because $\rho(\mathbf{r})$ varies over a length scale similar to λ (*i.e.* about 1 Å), the function $f(\mathbf{Q})$ decreases relatively quickly with increasing Q. Analytic approximations for $f(\mathbf{Q})$ have been calculated for all atoms and ions of interest using quantum mechanics. In general, the functions are qualitatively very similar, and a representative illustration is given above. The key idea is that the larger that atom or ion, then the narrower the atomic scattering function in reciprocal space. This is why neutron scattering has no appreciable Q-dependence: because the nucleus is so small, its Fourier transform is sufficiently broad to be considered constant over all accessible values of Q.

In our discussion of the concept of convolution, we made the point that a crystal lattice can be thought of as the convolution of a lattice of points with the contents of a single unit cell. When considering x-ray diffraction, we can extend this approach to consider the contents of a unit cell as the convolution of a set of point particles with the electron density functions for each point. This means that the Fourier transform of the crystal as a whole will be given by the Fourier transform of the lattice (*i.e.* the reciprocal lattice) multiplied by the transform of the unit cell contents as point particles, multiplied in turn by the transform of the electron density functions. It is this last aspect that is given by the atomic scattering factors. So, for x-rays, a general scattering formalism will be of the form:

$$F(hkl) = \sum_j f_j(Q_{hkl}) \exp[2\pi\mathrm{i}(hx_j + ky_j + lz_j)] \tag{36}$$

We can now see that the scattering from hydrogen atoms will necessarily be very small because $f(Q)$ will always be less than 1 ($= Z$). Also, heavy atoms — those with many electrons — will dominate the scattering because the corresponding values of $f(Q)$ may be many times larger than those for lighter atoms.

For comparison, the scattering formalism for neutron diffraction is of the form:

$$F(hkl) = \sum_j b_j \exp[2\pi\mathrm{i}(hx_j + ky_j + lz_j)], \tag{37}$$

where b_j is the "neutron scattering length" for the atom j — a quantity that describes how strongly that particular type of atom scatters neutrons. There is no systematic variation in the scattering lengths as a function of atomic size, and both positive and negative values are known; consequently, similarly sized atoms can actually scatter neutrons quite differently. This means that x-ray and neutron diffraction experiments emphasise different types of atoms differently, and this can be of enormous help in separating the scattering due to individual types of atoms, such as hydrogen.

For completeness, we will consider one other contribution to the scattering functions that is relevant to both neutron and x-ray diffraction patterns. That is the effect of thermal motion, which essentially acts to blur the position of each atom. To account for this, the position of each atom needs to be convoluted with the spread of displacements that arise from the thermal motion. Consequently, the Fourier transform of the unit cell incorporates the

Fourier transform of the spread of displacements as an additional multiplicative factor. If we assume that the thermal motion is isotropic and harmonic, then the Fourier transform of the spread of displacements (which for harmonic motion will be a Gaussian distribution) is given as

$$\begin{aligned} \mathcal{T}_j(\mathbf{Q}) &= \exp(-8\pi^2\langle u_j^2\rangle \sin^2\theta/\lambda^2) && (38)\\ &= \exp(-B_j \sin^2\theta/\lambda^2), && (39)\end{aligned}$$

where $\langle u_j^2\rangle$ is the mean-squared displacement of atom j, and B_j is commonly-used shorthand for the quantity $8\pi^2\langle u_j^2\rangle$. Because $\langle u_j^2\rangle$ is found to be proportional to temperature (except at low temperatures), this is usually called the "temperature factor", An alternative name is the "Debye-Waller factor", after the people who first developed the theory. So, taking into consideration the thermal motion, the x-ray structure factor becomes

$$F(hkl) = \sum_j f(Q_{hkl}) \exp[2\pi\mathrm{i}(hx_j + ky_j + lz_j)] \exp(-B_j \sin^2\theta_{hkl}/\lambda^2). \quad (40)$$

The primary effect of thermal motion on the diffraction pattern is to reduce the intensities of those reflections at large Q (large θ). As temperature increases, the displacement parameters B_j will increase, and the corresponding exponential term in equation (40) decreases, reducing the intensities further.

We are going to conclude our introduction to the theory of diffraction by returning to the idea that a diffraction experiment measures some quantity proportional to the square of the modulus of the structure factor; *i.e.*, $I(\mathbf{Q}) \propto |F(\mathbf{Q})|^2$. Despite the fact that we have lost much of the information contained within $F(\mathbf{Q})$, there is still merit in attempting a reverse Fourier transform using the intensities $I(\mathbf{Q})$ rather than the structure factors themselves.

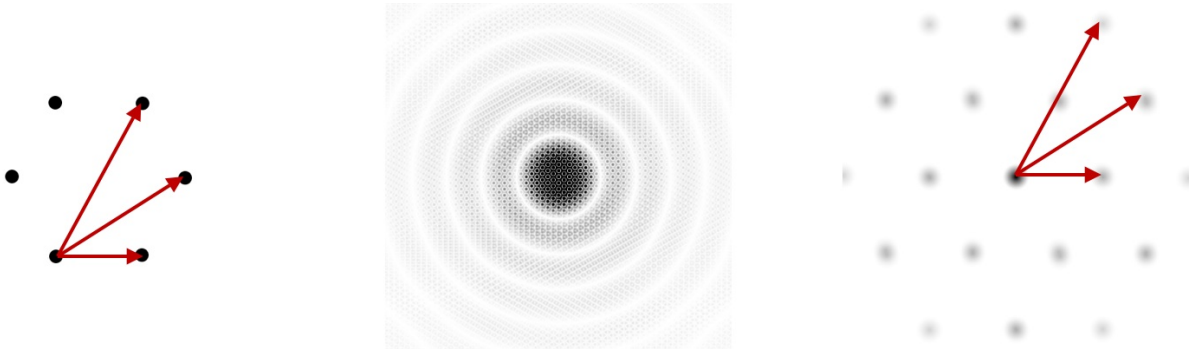

What we have illustrated in the figure above is a simple "molecule", containing six "atoms". The calculated values of $I(\mathbf{Q})$ are illustrated in the centre panel, and on the right hand side we see the reverse Fourier transform of this intensity information — a so-called "Patterson map". A Patterson map will contain a peak for each interatomic vector in the original structure. So here we have many more peaks than there are atoms in the molecule, but each peak can still be attributed to a pair of atoms in the molecule itself. We can see why

this works if we consider the mathematics involved (neglecting thermal motion or atomic scattering factors, for simplicity):

$$I(\mathbf{Q}) \propto |F(\mathbf{Q})|^2 = \left| \int \rho(\mathbf{r}) \exp(\mathrm{i}\mathbf{Q} \cdot \mathbf{r}) \, \mathrm{d}\mathbf{r} \right|^2 \quad (41)$$

$$= \int \rho(\mathbf{r}) \exp(\mathrm{i}\mathbf{Q} \cdot \mathbf{r}) \, \mathrm{d}\mathbf{r} \times \int \rho(\mathbf{r}) \exp(-\mathrm{i}\mathbf{Q} \cdot \mathbf{r}) \, \mathrm{d}\mathbf{r} \quad (42)$$

$$= \iint \rho(\mathbf{r}_j - \mathbf{r}_i) \exp[\mathrm{i}\mathbf{Q} \cdot (\mathbf{r}_j - \mathbf{r}_i)] \, \mathrm{d}\mathbf{r}_i \, \mathrm{d}\mathbf{r}_j. \quad (43)$$

So the intensities reflect information about the separations of all pairs of particles, rather than their absolute positions. It is these separations that we recover in a Patterson map. We will see in BL9 that this information is a useful starting point when attempting to solve a crystal structure from a diffraction pattern. In the mean time, however, we need to learn how to use symmetry to help us even more.

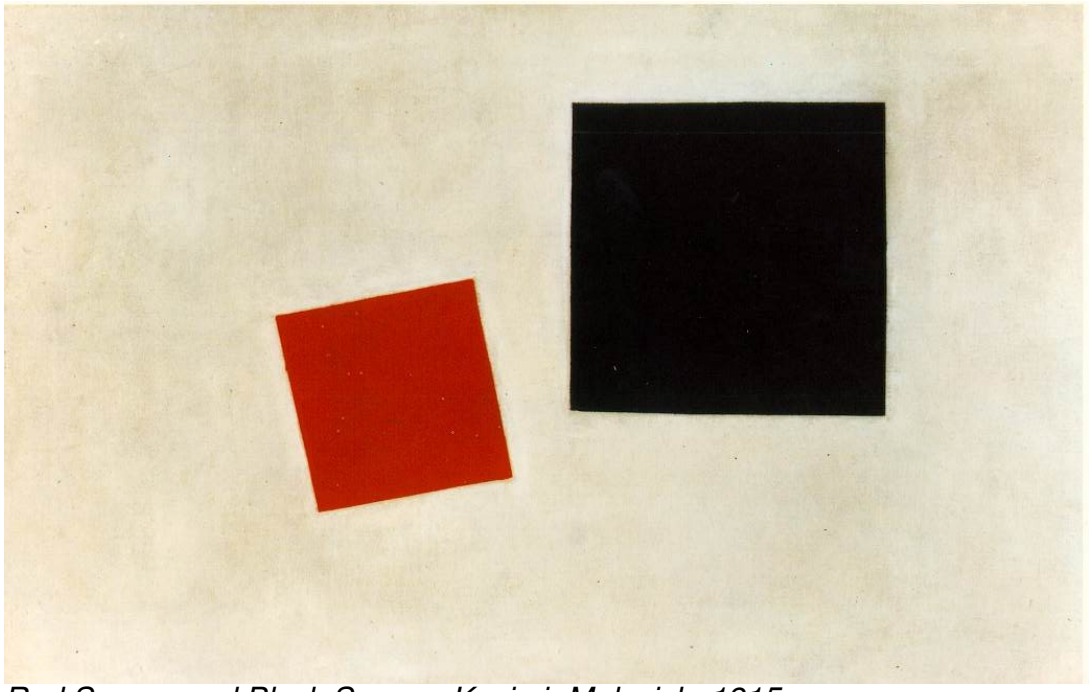

Red Square and Black Square, Kasimir Malevich, 1915

BL5: Point Symmetry

So far, we have studied how radiation is scattered from the atoms in any material. This has introduced the concept that the pattern of scattered radiation is given by the Fourier transform of the object, but with the loss of phase information. In this second half of the course, we are moving towards answering the inverse problem: given a measured diffraction pattern, how can we determine the structure of the crystal? This is a very difficult problem. The loss of phase information is the key hurdle to overcome. Our approach is to reduce the scale of the problem by making use of the symmetry of the crystal.

In this lecture, as in lectures BL6 and BL7, we will introduce some formal notions of crystal symmetry. We will explore point groups and space groups, with the view of understanding how symmetry of a crystal structure will affect the symmetry of a diffraction pattern.

We begin by considering the symmetry of points in space, with the view of applying our results to the symmetry of points within a crystal lattice. In determining the symmetry of a point, what we are asking is how we can rotate, reflect and/or invert the environment around the point such that it appears identical before and after the symmetry operations (*i.e.* comes into coincidence with itself). To see this more clearly, we consider each of the symmetry operations in turn.

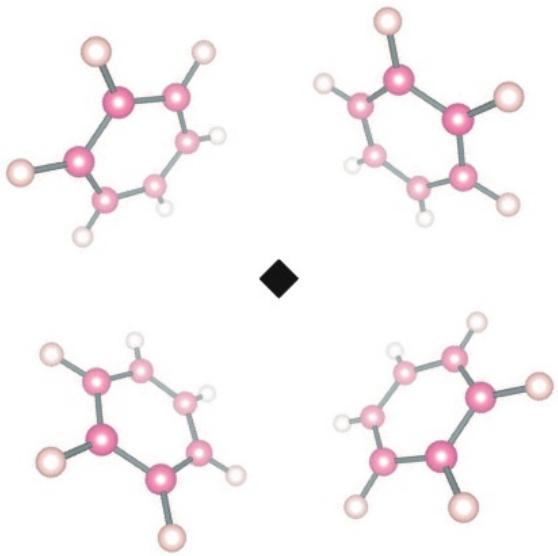

Rotational symmetry is present if an object comes into coincidence with itself after rotation by an angle of $360^\circ/n$ (where n is an integer) — in this case we say that the point has n-fold rotational symmetry. The diagram above illustrates a point with 4-fold rotational symmetry: each benzene molecule is mapped onto an identical neighbour after a rotation of 90°.

In crystallography, we need only deal with rotation axes with $n = 1, 2, 3, 4, 6$ (why?). There are a number of ways of representing the action of these symmetry elements. We will use two methods. The first is a simple mathematical approach, where we consider how each element would map the cartesian coordinates of a general point in space (x, y, z). For example, a 2-fold axis parallel to z will map (x, y, z) onto $(-x, -y, z)$; similarly, a 4-fold axis parallel to y will map (x, y, z) onto $(-z, y, x)$. It is a good exercise to convince yourself of these two examples, and also to go about writing down similar mappings for other rotation axes around the three cartesian axes. Practice makes perfect!

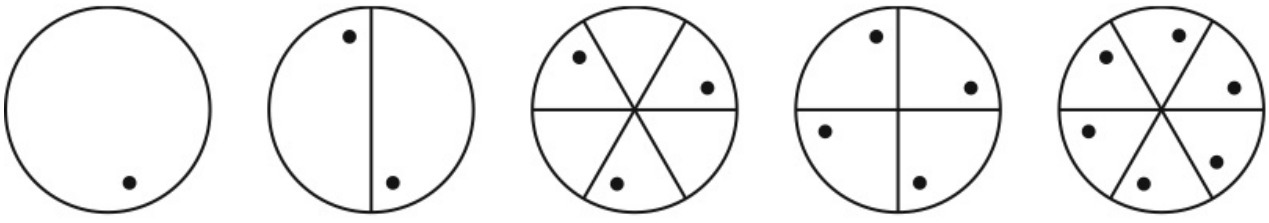

The second approach is a graphical one, where we construct so-called "sphere diagrams". The idea is that we view a sphere down a convenient axis (in this case, the rotation axis). We can draw as many lines as we like on these diagrams to indicate relevant planes (the actual choice will depend on the symmetry element(s) to be illustrated) — each line indicates where a single plane cuts the surface of the sphere. We start with a single point in an arbitrary position on the upper surface of the sphere, which we represent with a small filled circle. We then act on this point using our symmetry operation, recording each new place on the sphere to which the point is mapped. If the point is mapped to another position on the upper surface of the sphere, then we use another small filled circle to represent this;

if the point is mapped to a position on the opposite side of the sphere, then we illustrate this with a slightly larger, open circle. We apply the same symmetry operation to the new point, and continue drawing each new point until we have returned to our original starting place. The trace of points on the surface of the sphere then represents our particular symmetry operation.

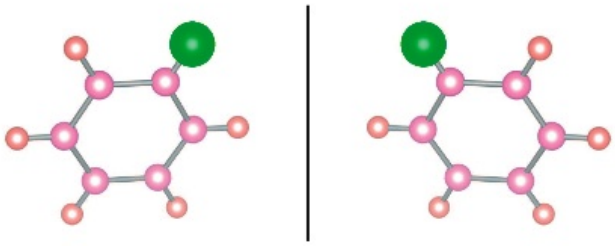

Mirror planes are just as intuitive: if the environment around a point can be reflected through a plane and come into coincidence with itself then we say that the system has mirror symmetry (an example is shown above). In crystallographic systems, an object can have one, two or three independent mirror planes (which must lie by orthogonal); however, when these are combined with rotational symmetry axes there can be additional mirror planes at angles of 45° and 60°. In terms of cartesian coordinates, a mirror plane perpendicular to x will reflect (x, y, z) onto $(-x, y, z)$. When it comes to representing mirror planes on sphere diagrams, we use bold lines. If the circle itself is bold, this represents a mirror plane that cuts the sphere at the "equator" — a mirror plane coincident with the sheet of paper.

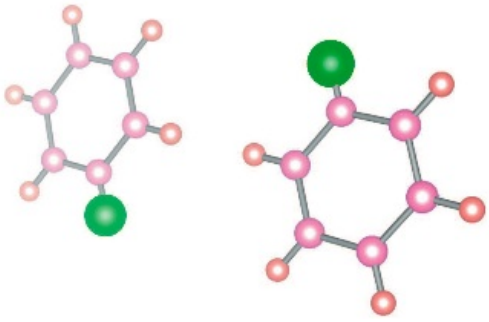

Another point symmetry element is a so-called "centre of symmetry", or "inversion" element, which exists if for every point at position (x, y, z) there is an identical point at $(-x, -y, -z)$. An example is the pair of chlorobenzene molecules above, where the centre of symmetry lies at the midpoint of the two molecules. A crystal with a centre of symmetry is called "centrosymmetric"; one without a centre of symmetry is called "acentric". There is no explicit method of representing a centre of symmetry on a sphere diagram, but we can still show its existence via its effect on the points already drawn (more about this in a moment).

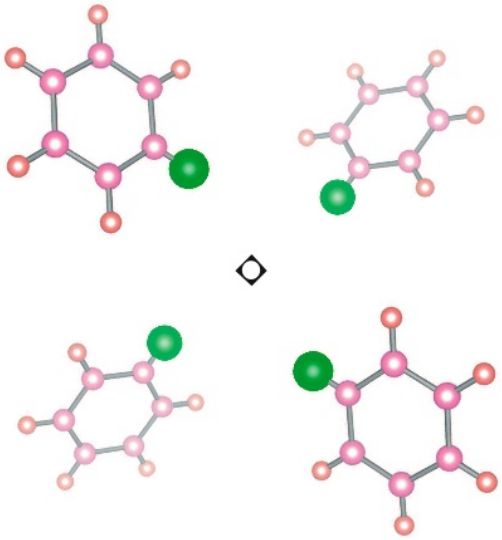

The final type of point symmetry to consider is actually a combination of two other symmetry elements: namely a rotation axis and a centre of symmetry. The result is called a "rotoinversion" axis (older texts may refer to an "improper rotation axis"), and it acts in the following way. First, the object is rotated by an angle of $360^\circ/n$ (as for the usual rotation axis), but then inversion symmetry is applied to transform the new point to its inverse. An example of a $\bar{4}$ axis is shown above (the bar above the number tells us this is a rotoinversion axis); we leave the cartesian representations of these rotoinversion operations as an exercise. Note that a $\bar{1}$ axis is just a fancy way of writing a centre of symmetry — the initial rotation of 360° is trivial, so all we are left with is the inversion itself.

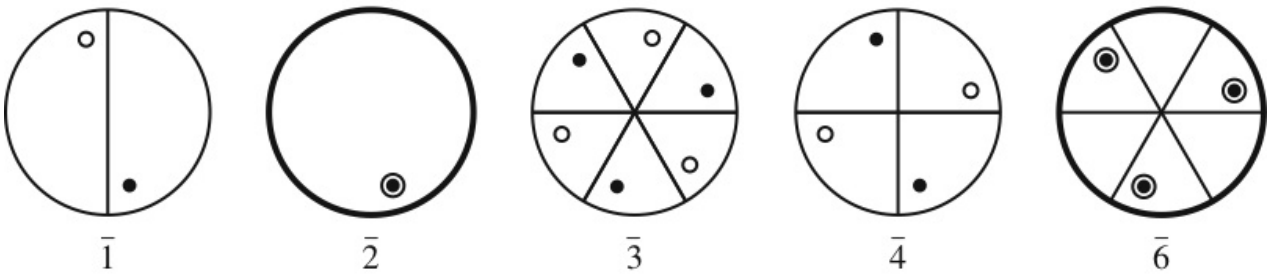

Here are the sphere diagrams for the rotoinversion axes. One thing to note, and the generality of this observation will become more apparent with time, is that sometimes one symmetry operation, or a group of symmetry operations, can produce other symmetry operations, essentially without us asking for them. For example, the $\bar{2}$ axis generates a mirror plane perpendicular to the axis (in fact, the two operations are indistinguishable). The same happens for the $\bar{6}$ axis. More subtly, perhaps we can see that the $\bar{3}$ operation also includes both a 3 axis and an inversion centre; a $\bar{4}$ axis includes a 2-fold rotation axis. And so on.

This leads us to consider the various ways in which symmetry operations can combine. What often happens is that as we start to combine individual symmetry operations, we automatically produce others in the process. Whenever we find a self-contained set of

symmetry operations, we call the set a "group" — in fact, a "point group" if all the symmetry elements are point symmetry operations.

For example, when a rotation axis is normal to a mirror plane, we can write the combined set of operations as n/m (n still referring to the order of the rotation axis, and $/m$ designating a mirror plane exists, and is perpendicular to the rotation axis). Let us consider what this means for some different values of n:

(i) $1/m$ is just a mirror plane around the "equator" — precisely the same as $\bar{2}$ or m.

(ii) $2/m$ is a new group that we can add to our list of point symmetries.

(iii) $3/m$ gives a sphere diagram identical to that for $\bar{6}$, and so the two are identical groups. We use the $\bar{6}$ notation in preference, because it reflects the highest-order rotation axis for this group.

(iv) $4/m$ is another new group ...

(v) ... as is $6/m$.

It is a good exercise to repeat this process for the rotoinversion axes, and to decide which combinations give new groups, and which are already accounted for. If we start to add mirror planes that *include* the rotation axis, and/or rotation axes perpendicular to the primary axis, then we can generate even more groups.

Fortunately, the number of possible groups is not immense. Well, it would be infinite — except that the translational symmetry of a crystal lattice restricts the number of crystallographic point groups to just 32. The labels for these are given in the table below; some of these (*e.g.* $\bar{6}$ and $2/m$) should already be familiar.

Crystal system	**Symmetry requirements**	**Point groups**				
Triclinic	None	1	$\bar{1}$			
Monoclinic	One 2-fold axis	2	m	$2/m$		
Orthorhombic	Three 2-fold axes	222	$mm2$	mmm		
Trigonal	One 3-fold or $\bar{3}$ axis	3	$\bar{3}$	32	$3m$	$\bar{3}m$
Tetragonal	One 4-fold or $\bar{4}$ axis	4 $\bar{4}2m$	$\bar{4}$ $4/mmm$	$4/m$	422	$4mm$
Hexagonal	One 6-fold or $\bar{6}$ axis	6 $\bar{6}m2$	$\bar{6}$ $6/mmm$	$6/m$	622	$6mm$
Cubic	Four 3-fold or $\bar{3}$ axes	23	$m3$	432	$\bar{4}3m$	$m\bar{3}m$

It will be evident that we have associated each of these point groups with one of the seven different crystal systems — the seven types of unit cell we introduced in lecture BL2. This is because the existence of a certain type of point symmetry will demand a certain level

of lattice symmetry. For example, it will be impossible to have a 4-fold axis in a crystal structure if each of the three unit cell axes have different lengths, or the angles between them are not 90°. We list in the table the minimum symmetry requirements for each of the seven crystal systems. It is worth committing these to memory!

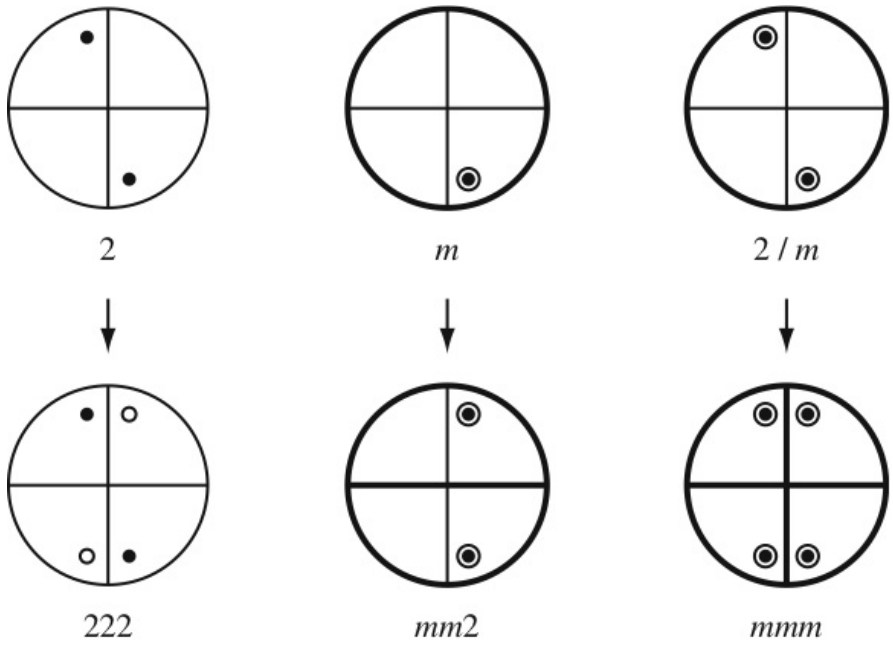

An instructive exercise is to consider how higher-symmetry point groups can be generated by adding symmetry elements to lower-symmetry point groups. For example, the addition of a horizontal 2-fold axis to each of the monoclinic point groups generates the corresponding orthorhombic point groups. It is important to note that in these cases the existence of symmetry operations involving two directions has automatically generated symmetry along the third direction.

Point groups with symmetry elements along more than one axis are given multiple components to denote the symmetry elements along each direction. For convenience some point groups are given an abbreviated symbol when this abbreviation implies additional symmetry (*e.g.* when we used $\bar{6}$ to represent $3/m$, above). In the case of the orthorhombic groups, the symbol mmm still implies the existence of the three 2-fold axes that are automatically generated by the three perpendicular mirror planes.

As an exercise, what are the point groups of the various molecules in the following picture?

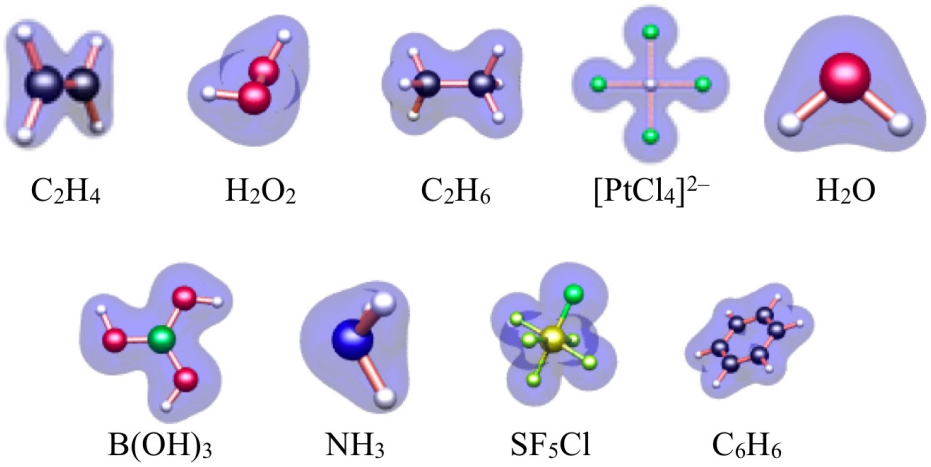

Actually, point groups provide a representation of symmetry on all length scales. We can think of a point group representing the symmetry of a gemstone, or the relationship between anisotropic physical properties and the crystal axes. We can consider the point group of a crystal structure, and also of specific sites within the crystal structure. We can even use point groups to represent the symmetry of diffraction patterns.

Crystal system	**Laue class**	**Point groups of the Laue group**			
Triclinic	$\bar{1}$	1	$\bar{1}$		
Monoclinic	$2/m$	2	m	$2/m$	
Orthorhombic	mmm	222	$mm2$	mmm	
Trigonal	$\bar{3}$	3	$\bar{3}$		
	$\bar{3}m$	32	$3m$	$\bar{3}m$	
Tetragonal	$4/m$	4	$\bar{4}$	$4/m$	
	$4/mmm$	422	$4mm$	$\bar{4}2m$	$4/mmm$
Hexagonal	$6/m$	6	$\bar{6}$	$6/m$	
	$6/mmm$	622	$6mm$	$\bar{6}m2$	$6/mmm$
Cubic	$m3$	23	$m3$		
	$m\bar{3}m$	432	$\bar{4}3m$	$m\bar{3}m$	

The question then arises of how the symmetry of an object is related to the symmetry of its diffraction pattern. Here there are two results. The first is that all of the point symmetry elements of the object are preserved in the Fourier transform. The second result builds on an observation we made in the very first lecture, where we noticed that — even in the absence of any symmetry in real-space — the Fourier transform had a type of inversion symmetry. Specifically, the Fourier components $F(\mathbf{Q})$ and $F(-\mathbf{Q})$ were related by complex conjugation. Since, in a diffraction experiment, we measure something proportional to $|F(\mathbf{Q})|^2$, actually the intensities $I(\mathbf{Q})$ and $I(-\mathbf{Q})$ are identical. Hence a diffraction pattern

for a crystal will be left unchanged if we map each point (h, k, l) onto its inverse $(-h, -k, -l)$ — the definition of a centre of symmetry. So we are left with the result that the point symmetry of a diffraction pattern is given by the point symmetry of the crystal *plus* an inversion centre. Every diffraction pattern is centrosymmetric, belonging to one of only 11 possible point symmetries, called the "Laue classes".

We finish with one simple example to illustrate that the point group symmetries are at least preserved in a diffraction experiment. Imagine we have a system that possesses a 2-fold axis parallel to z, running through the origin. Then we can divide all the atoms in our system into three groups. The first group contains all those atoms that lie on the axis itself, and we know that these will have coordinates $(0, 0, z)$. We then divide the remaining atoms into two equal groups such that each atom in one group will be mapped onto an atom in the second group by the 2-fold axis. That is, for each atom at (x, y, z), we know that there is an equivalent atom at $(-x, -y, z)$, and we place one atom in our second group, and one atom in our third group.

Now, let us consider an arbitrary point in reciprocal space (h, k, l). We will show that the Fourier component at this point is the same as that at $(-h, -k, l)$, and hence the diffraction pattern will also contain a 2-fold axis, this time lying perpendicular to $\mathbf{c}^*$.

$$
\begin{aligned}
F(hkl) &= \sum_j f_j \exp[2\pi\mathrm{i}(hx_j + ky_j + lz_j)] && (44)\\
&= \sum_{j\in\text{group1}} f_j \exp[2\pi\mathrm{i}(lz_j)] + \sum_{j\in\text{group2}} f_j \exp[2\pi\mathrm{i}(hx_j + ky_j + lz_j)] \\
&\quad + \sum_{j\in\text{group3}} f_j \exp[2\pi\mathrm{i}(-hx_j - ky_j + lz_j)] && (45)\\
&= \sum_{j\in\text{group1}} f_j \exp[2\pi\mathrm{i}(lz_j)] + \sum_{j\in\text{group2}} f_j \exp[2\pi\mathrm{i}((-h)x_j + (-k)y_j + lz_j)] \\
&\quad + \sum_{j\in\text{group3}} f_j \exp[2\pi\mathrm{i}(-(-h)x_j - (-k)y_j + lz_j)] && (46)\\
&= F(\bar{h}\bar{k}l) && (47)
\end{aligned}
$$

(here, the notation $(\bar{h}\bar{k}l)$ is shorthand for $(-h, -k, l)$).

We now know how to characterise the symmetry about a point, and have shown how the point symmetries of an object and its Fourier transform are related. When it comes to considering a crystal lattice, however, we have an additional consideration in that there are infinitely many equivalent points within the crystal. In BL6, we concern ourselves with symmetry operations that map equivalent points onto one another: the translational symmetry elements.

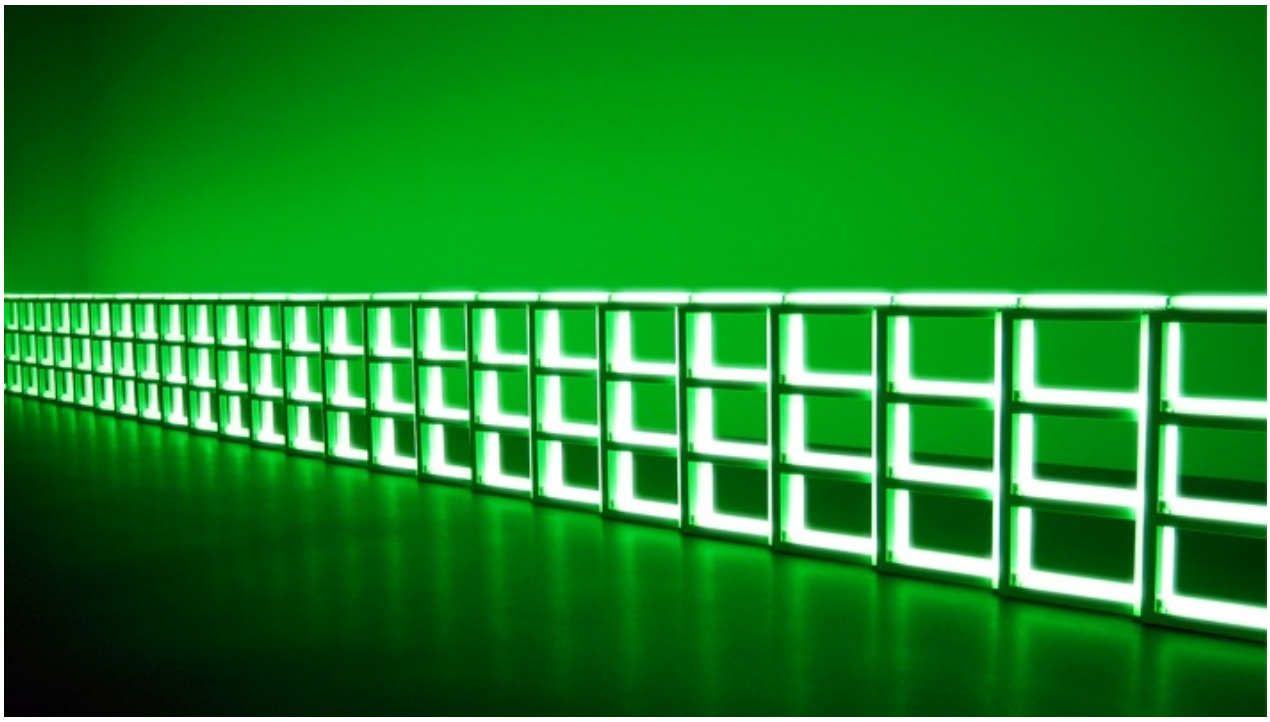

Untitled, Dan Flavin, 1973

BL6: Translational Symmetry

There can be no translational element to point symmetry, since by its very definition any point symmetry must map the origin onto itself. But in a crystal lattice we have an infinite array of equivalent points, and it becomes necessary to consider what sorts of symmetry elements can relate these to one another.

The simplest such operation is of course that of translation along the lattice vectors themselves. We already know that these map lattice points onto lattice points, so they certainly must leave the structure invariant. A slightly more subtle version of this same idea is where we have what we call a "centred" or non-primitive lattice; that is, where the unit cell contains more than one lattice point. Seven of the 14 different "Bravais lattices" (see illustration overleaf) are primitive lattices, but seven are centred lattices. We have already met the primitive members of this family, and (hopefully) the concepts of C-centred, body-(I-)centred and face- (F-)centred lattices should be familiar from IA. We are not going to worry about the less-familiar "rhombohedral" centreing of trigonal lattices, except to note that it exists and is given the symbol R. The key point is that, just as lattice translations are a type of translational symmetry, so too are translations between lattice points on a centred unit cells. The translations themselves can be written explicitly in terms of cartesian coordinates. For example, the operation one might call "face-centreing" corresponds to mapping each point (x, y, z) onto $(x + \frac{1}{2}, y + \frac{1}{2}, z)$, $(x + \frac{1}{2}, y, z + \frac{1}{2})$ and $(x, y + \frac{1}{2}, z + \frac{1}{2})$.

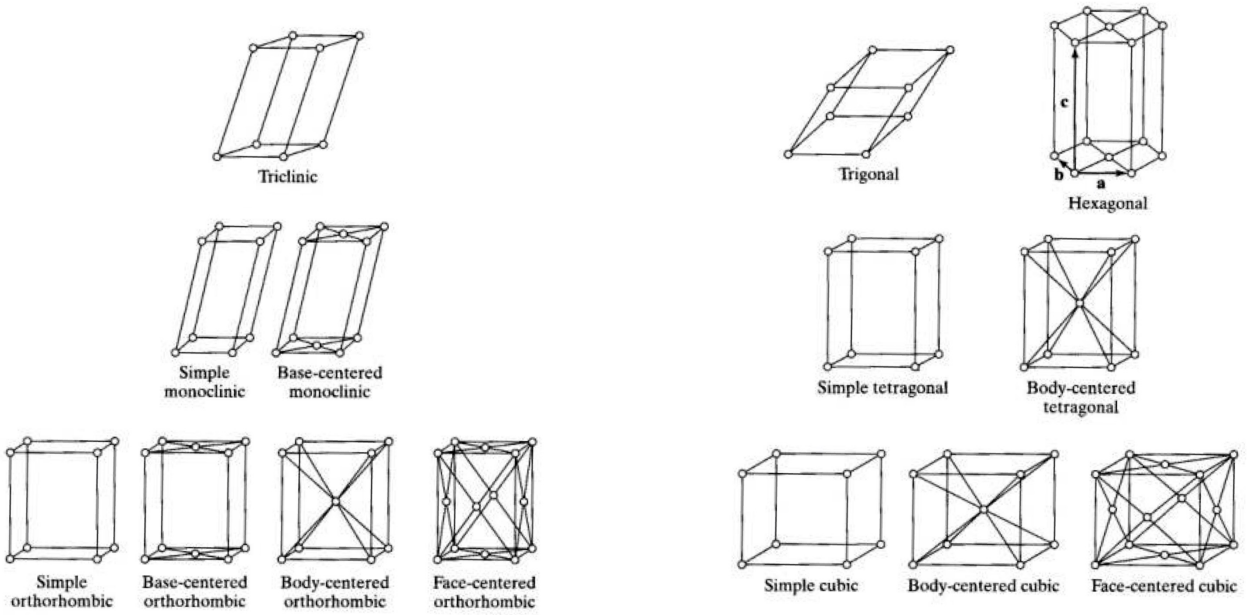

There are two general points to make about centred lattices while we are discussing them. The first is to ask why we need centred lattices at all. It is true that every centred lattice could be described by a smaller primitive unit cell — a face-centred cubic lattice has a rhombohedral primitive unit cell, for example (see if you can find it). But we invoke the notion of lattice centreing so that the unit cell correctly reflects the actual symmetry of the crystal. A face-centred cubic lattice has cubic symmetry, not rhombohedral symmetry, so we need a cubic unit cell. OK, so centreing is a good thing and should be allowed. But then we notice that there are some centred lattices "missing" from our 14 Bravais lattices — there is no face-centred monoclinic lattice nor, for example, any C-centred tetragonal lattice. This is because we only invoke the minimum number of different centred lattices necessary for each crystal system. We can always choose different axes such that a face-centred monoclinic lattice can be described as C-centred monoclinic; a C-centred tetragonal lattice is actually primitive tetragonal in another setting. It is a good exercise to convince oneself of these equivalences.

Our next step is to consider the combination of translational and point symmetry elements. The idea here is that translation from one lattice point to another is broken up into equal segments: each segment combines a partial translation with a point symmetry operation, such as rotation or reflection. If the number of segments is appropriate, then by the time the point symmetry operation has returned us to its own starting point, the translations will have moved us to the next lattice point. Let us be more explicit about this by considering the two types of combinations possible.

A screw axis is present when a rotation of $360^\circ/n$, combined with a relative translation of m/n along a lattice vector, brings the crystal back into coincidence with itself. The label m here is simply an integer, chosen such that $0 < m < n$; in particular, it does not refer to a mirror plane. Such a screw axis would be labelled as n_m. An example of a 2_1 screw axis is shown below. The axis works by coupling a rotation of 180° to a translation of a half a unit cell. After two operations, we have completed a full revolution and a full lattice translation.

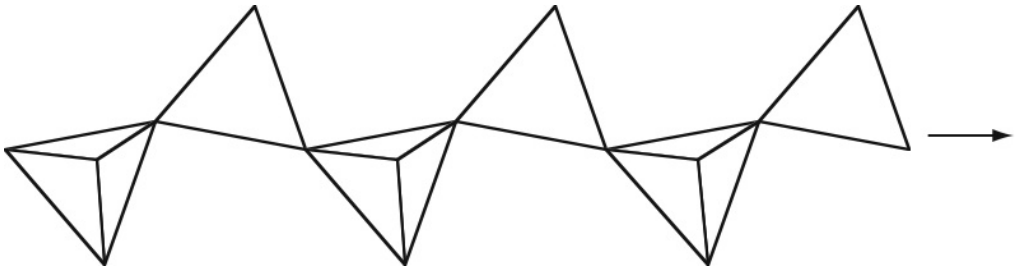

Using cartesian coordinates to describe a 2_1 axis parallel to z, we would say that the point (x, y, z) is mapped first to $(-x, -y, z)$ and then, after being translated a half a unit cell along z, ends up at $(-x, -y, z + \frac{1}{2})$. A second application of the same operation would take this new point to $(x, y, z + 1) \equiv (x, y, z)$ as required.

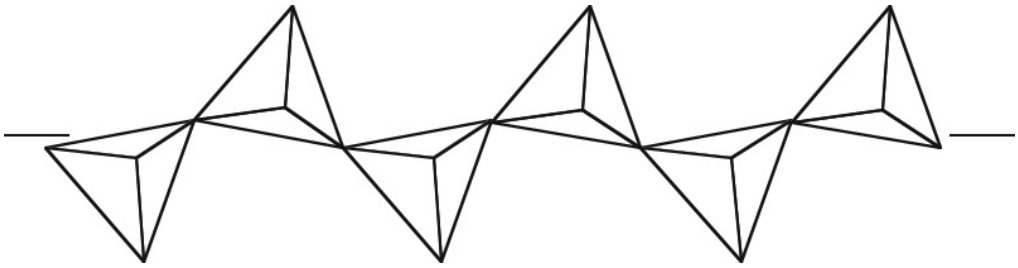

The combination of partial lattice translations with a mirror plane gives a so-called "glide plane". Because a mirror operation has an order of only 2, the translations involved must always correspond to one half of a lattice vector. We denote a glide plane by the axis along which this translation occurs. So, an a-glide corresponds to a translation of $\mathbf{a}/2$ with each operation. It is not difficult (and a good exercise) to show that the only non-trivial mirror planes one can associate with these translations must include the axis itself. So an a-glide must involve reflection perpendicular to y or to z, but will never involve reflection perpendicular to x. The example illustrated above involves translations along a horizontal direction, coupled with reflection through a plane that lies horizontally and perpendicular to the sheet of paper. If we were to label the horizontal axis as x, the vertical axis as y, and imagined the axis z to be projected into the plane of the paper, then we would call the glide plane an a-glide perpendicular to ("on") b. In terms of cartesian coordinates, we would have the translation from (x, y, z) to $(x + \frac{1}{2}, y, z)$ followed by a reflection to $(x + \frac{1}{2}, -y, z)$.

There are two other (slightly odd-looking) types of glide plane that follow the same principles. An n-glide involves a translation along a cell diagonal, such as along $(\mathbf{a} + \mathbf{c})/2$. A d-glide, so-named because it occurs in the crystal structure of diamond, involves translations of either $(\mathbf{a} \pm \mathbf{b} \pm \mathbf{c})/4$ or $(\mathbf{a} \pm \mathbf{b})/4$, depending on the specific crystal symmetry involved. In each case, the translations involved are always half a vector between two lattice points.

So now we have enumerated all the possible symmetry elements that one can hope to find in a crystal structure. Rotations, reflections, rotoinversions, a centre of symmetry, lattice translations, screw axes and glide planes. The point symmetry operations are preserved in the diffraction pattern, and we always end up with a centre of symmetry — even if the

original object is acentric. The lattice translations will be reflected in the spacing of the reciprocal lattice. But the combined translational and point symmetries — the glide planes and screw axes — leave a much subtler influence on the diffraction pattern, and we will return to this in lecture BL8.

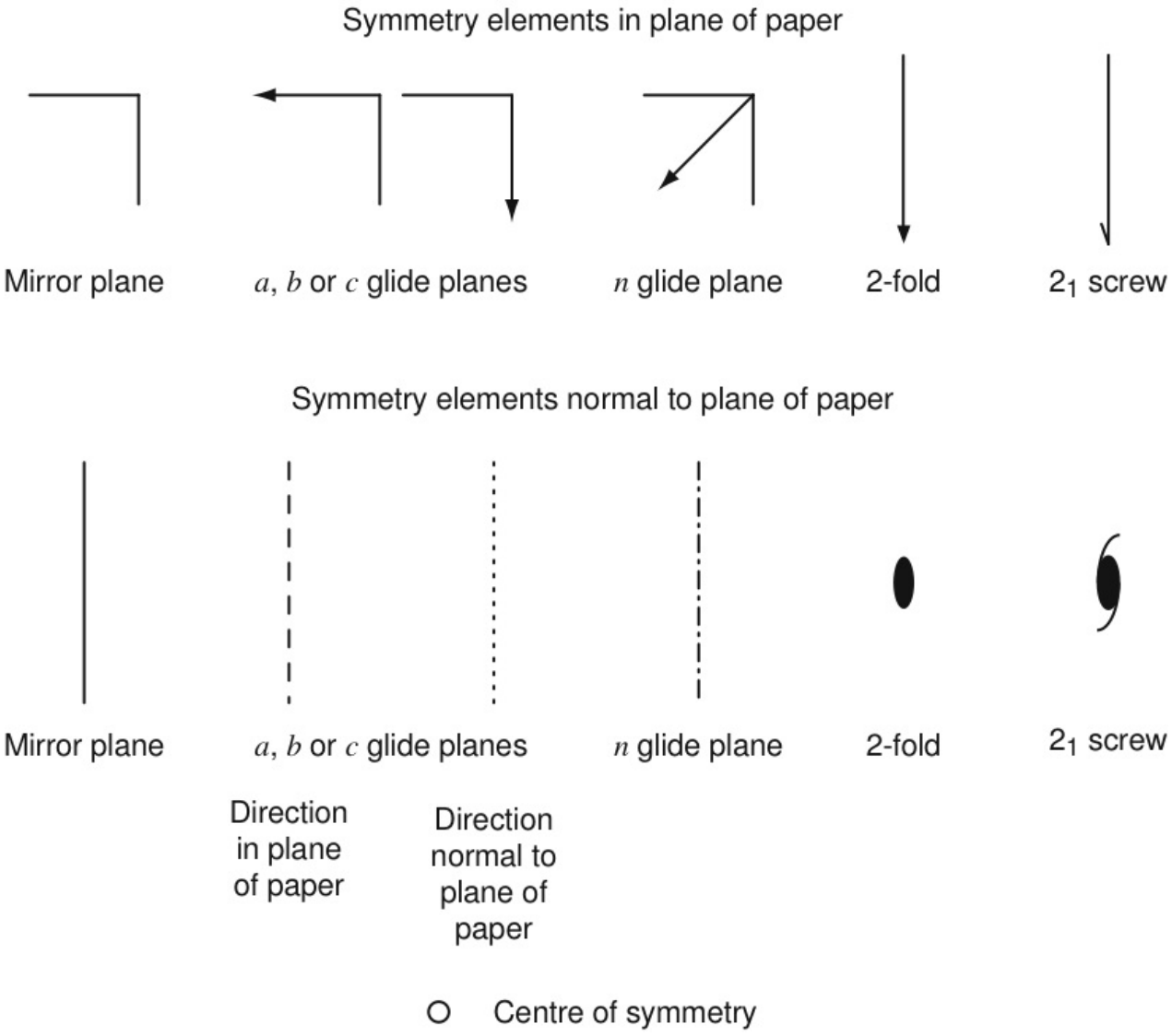

One of the key skills we need to develop in this course is that of recognising symmetry elements in crystal structures. Typically, we are going to be shown a plan of a crystal structure, and we need to be able to indicate on that plan what symmetry elements exist, and where they operate in three dimensions. To this end, we will use a number of different symbols, some of which are illustrated above. One example is the structure of andalusite, a mineral which contains aluminium, silicon and oxygen atoms. A plan of its structure — first left unmarked, and then with all symmetry elements included — is given overleaf. Aluminium atoms atoms are represented as small open circles, silicon atoms as small filled circles and oxygen atoms as large open circles. In the diagrams, we are looking down one of the crystal axes. It should be possible to see individual SiO_4 and AlO_4 tetrahedra (hint: in both cases, two of the O atoms lie on top of one another in this projection).

We will work through a different, but similar, example in class itself.

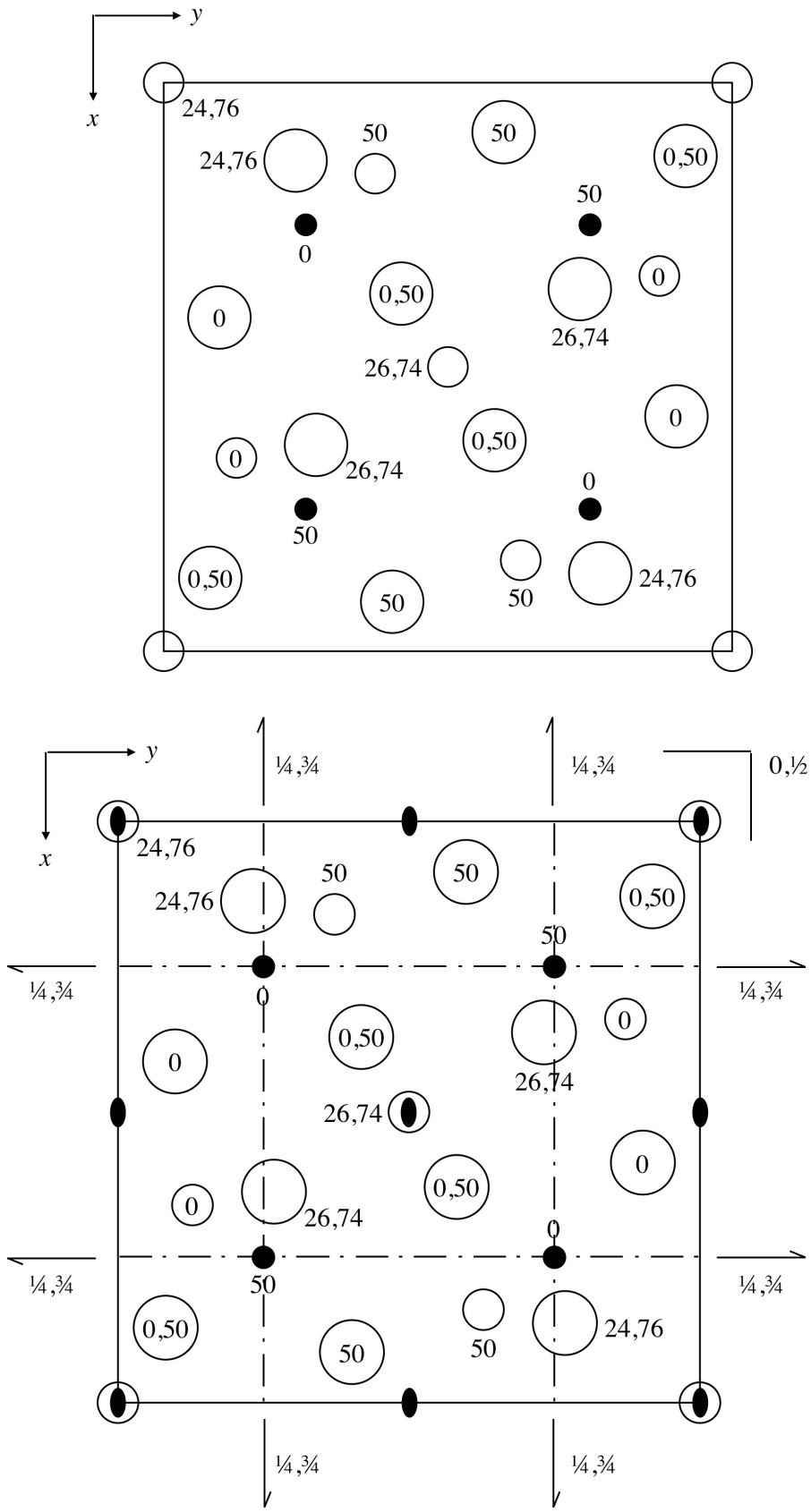

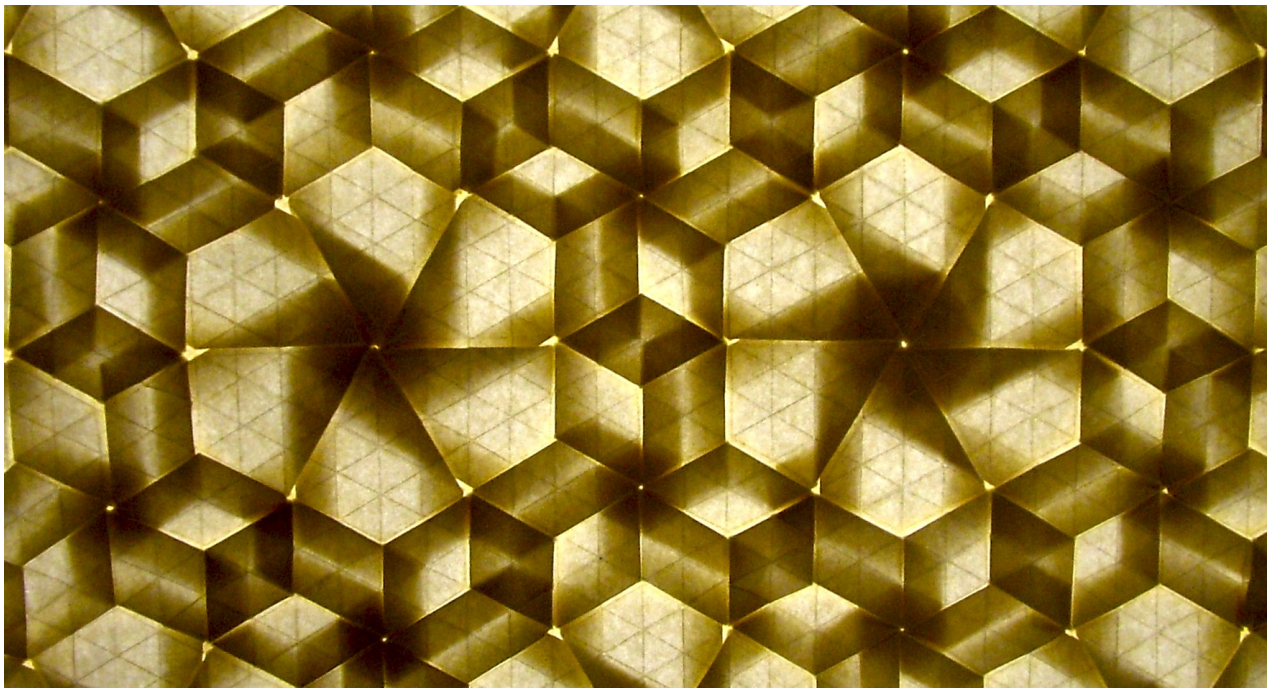

Deltoidal Trihexagonal Tiling + Stars = Crazy Delicious, Eric Gjerde, 2006

BL7: Space Groups

In lecture BL5, when we discussed point group symmetries — rotations, reflections, inversions and rotoinversions — we showed that different possible combinations could be collected into a series of 32 self-contained groups, which we called the "point groups". The very same concept can be applied to the combinations of point group and translational symmetry operations, allowing us to enumerate each of the 230 possible "space groups".

This is a very large number of groups — far more than we can hope to cover in any real detail. But it is useful to see from where this number of 230 arises. The first step in enumerating the space groups is to merge the point groups with each of the 14 Bravais lattices — essentially here we are considering just the simplest form of translational symmetry, namely the lattice translations themselves. Note that we can only merge point groups with Bravais lattices of the corresponding crystal symmetry. So the three monoclinic point groups 2, m and $2/m$ can only be merged with the two monoclinic Bravais lattices (P-monoclinic and C-monoclinic), giving six possible monoclinic space groups. If we do this same process for all seven crystal systems then we obtain 61 space groups, as shown in the table overleaf.

We use a very intuitive system for labelling each of these space groups: we simply prefix the original point group by the centreing of the corresponding lattice. Because the crystal symmetry of the point group is known in each case, then there is no ambiguity as to the particular Bravais lattice involved. So, for example, the six monoclinic point groups described above would be given the symbols $P2$, Pm, $P2/m$, $C2$, Cm and $C2/m$.

Crystal system	Possible centreing	Number of point groups	Number of resultant space groups
Triclinic	P	2	2
Monoclinic	P, C	3	6
Orthorhombic	P, I, C, F	3	12
Trigonal	P, R	5	10
Tetragonal	P, I	7	14
Hexagonal	P	7	7
Cubic	P, I, F	5	15

The next step is to consider the various combinations of point groups with screw axes and glide planes. Taking the primitive monoclinic space groups $P2$, Pm and $P2/m$ as an example, we can obtain these new combinations by replacing 2-fold axes by 2_1-screw axes, and/or by replacing mirror planes by glide planes [it turns out that we can always choose a set of axes such that any glide plane can be thought of as a c-glide (rather than, *e.g.* an a- or n-glide)]. Putting these options together we obtain the eight primitive monoclinic space groups:

P	1	2	2_1
1		$P2$	$P2_1$
m	Pm	$P2/m$	$P2_1/m$
c	Pc	$P2/c$	$P2_1/c$

When we take the same approach to the C-centred monoclinic lattice, we find that some of the new space groups are not unique (much as we found that *e.g.* the point groups $3/m$ and $\bar{6}$ were identical). In particular, the combination of C-centreing and a 2-fold rotation axis automatically generates a set of 2_1 axes, so that the point groups $C2$ and $C2_1$ are indistinguishable, giving a total of five C-centred monoclinic space groups ($C2$, Cm, Cc, $C2/m$ and $C2/c$).

To see the equivalence between $C2$ and $C2_1$ more clearly we are going to introduce the concept of space group diagrams, which are similar in some ways to the sphere diagrams we used for point groups, and similar also to the plans of unit cells we looked at in BL6. The idea is to represent a given space group by the set of points produced when the series of space group symmetries are applied to a single arbitrary point. We start with a plan of the unit cell. This need not be to scale but should represent the fundamental crystal symmetry of the space group in question. Since, at this point, we are trying to illustrate the properties of the monoclinic space group $C2$, we choose a plan that illustrates the monoclinic symmetry: this is best done by viewing the unit cell down the $\mathbf{b}$ axis (the unique

axis, perpendicular to both $\mathbf{a}$ and $\mathbf{c}$). To emphasise that the angle β need not be $90°$, we give this an arbitrary value, such as in the diagram below.

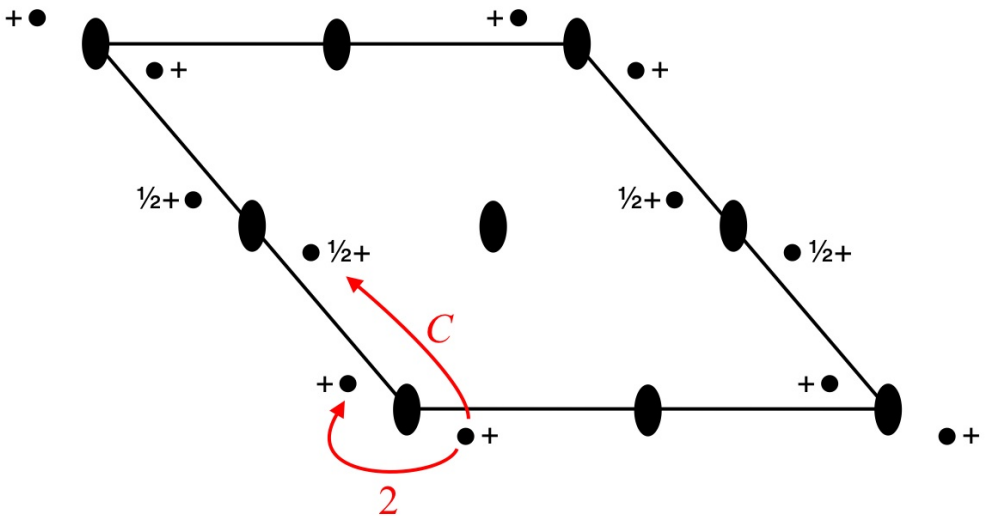

We then represent an arbitrary single point, which — as for the sphere diagrams — we illustrate as a small filled circle. A plus sign is shown next to the point to indicate that it lies somewhere above the $y = 0$ plane. We then apply each of the space group operations, recording the positions to which these map our original point. Each successive operation is applied to *all* such positions, so that we can obtain the cumulative effect of multiple operations. If a given operation causes us to move outside the original unit cell, we simply copy the position to a corresponding point within the unit cell (allowed because we know that lattice translations are symmetry operations in their own right), and continue from there. For each translational or point symmetry element we use, we indicate the operation using the symbols given in BL6.

So, for $C2$, starting from a single arbitrary point, we find that the C operation gives us a second position; the 2-fold axes then produce two new positions again. In general, what we find is that the total number of distinct related positions within a single unit cell is given by the number of positions in the corresponding point group (in this case 2, because the point group 2 has two independent positions), *multiplied by* the number of lattice points in the unit cell (in this case also 2 because C-centreing gives 2 lattice points per unit cell). We call these "general equivalent positions", of which there are 4 in the present example.

Once we have found as many general positions as we expected based on the centreing and the point group symmetry, we can then proceed to look for other symmetry elements that may have been produced in the process. In this particular case we find that there is a set of 2_1 screw axes that are parallel, but not coincident, with the 2-fold axes from which we started. These have been highlighted in the diagram overleaf. It is straightforward to show that if we had started with a set of 2_1 axes with the same C-centreing, then we would obtain the 2-fold rotation axes for free as well. By convention we use the symbol $C2$ rather than $C2_1$ (since the former more readily represents the corresponding point group symmetry), but the point is that both are equivalent.

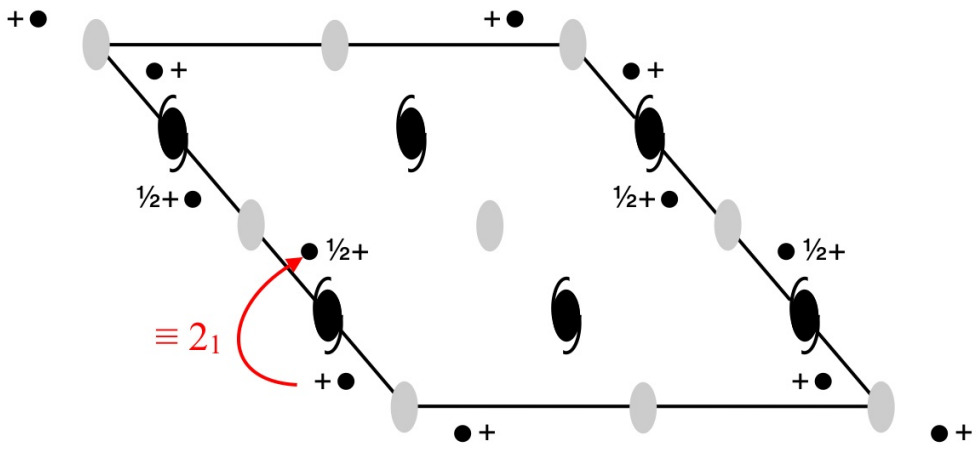

With other crystal systems there are many other examples where the application of some symmetry operations automatically generates other symmetry operations, just as with point groups. The total number of independent space groups is then 230, distributed across the crystal systems as given in the table below.

Crystal system	P	I	C	R	F	**Total**
Triclinic	2	–	–	–	–	2
Monoclinic	8	–	5	–	–	13
Orthorhombic	30	9	15	–	5	59
Trigonal	18	–	–	7	–	25
Tetragonal	49	19	–	–	–	68
Hexagonal	27	–	–	–	–	27
Cubic	15	11	–	–	10	36

In this course we are going to focus primarily on the monoclinic space groups and the orthorhombic space groups. We have already met all of the 13 monoclinic space groups, and it should be a straightforward exercise to draw space group diagrams for each of these.

The orthorhombic space groups are greater in number, but not very much more complicated. In each case, the space group symbol starts with a designation of the type of centered lattice — in this case, P, C, I and F are all possible. This is followed by three characters, which will be some variation on one of the three orthorhombic point groups 222, $mm2$ and mmm. The rules are the same as for the monoclinic systems: we can replace 2-fold axes by 2_1 axes, and mirror planes by glide planes. The particular position within the space group symbol tells us about the particular crystal axis (or corresponding perpendicular plane) with which we are concerned. This is all seen most easily with an example.

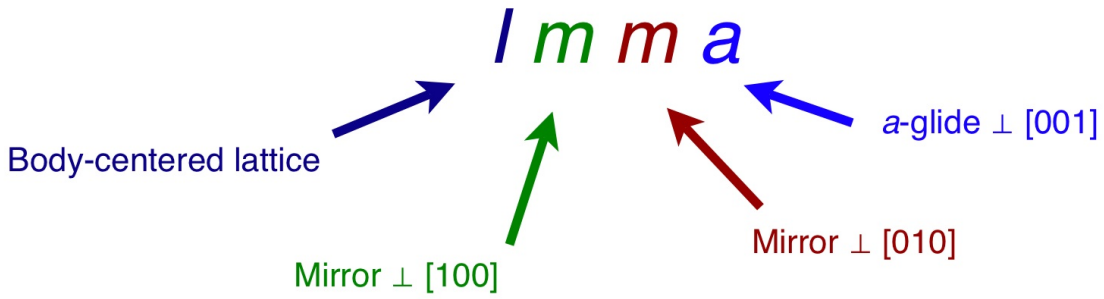

Our example is the space group symbol $Imma$. The first character I tells us that this is a body-centred space group. We then recognise the next three characters, mma, as a variation on the point group mmm. This tells us a number of things. First, that the space group is an orthorhombic space group — we know this because we know mmm is an orthorhombic point group. We say that the "point group of the space group $Imma$ is mmm". This is going to tell us about the point group symmetry of the diffraction pattern. Then, because mmm is a centrosymmetric point group, we now know that $Imma$ is a centrosymmetric space group.

But we can break down the "mma" portion of the space group symbol even further. The first "m" tells us that there are mirror planes perpendicular the $\mathbf{a}$ axis; the second "m" that there are mirror planes perpendicular to the $\mathbf{b}$ axis; the final "a" that there are a-glides perpendicular to the $\mathbf{c}$ axis. So the "a" symbol itself tells us about the direction of the translations associated with these glide planes, but the orientation of the glide planes is indicated by the position of the "a" label within the space group symbol. $Imam$, for example, would contain a-glides perpendicular to the $\mathbf{b}$ axis.

At this point, let us make a point about the uniqueness of crystal axes. For a monoclinic crystal, it makes real sense to label one of the axes as $\mathbf{b}$, because there is only one axis that is perpendicular to the other two. But in orthorhombic systems the choice is not unique. Instead the labelling is arbitrary, although the crystallography community has arrived at some conventions to avoid counting space groups twice. These are the same sorts of conventions that tell us there is no point having body-centred monoclinic lattices, and so on. All things considered, what this means in practice is that two people might arrive at two different space group labels to describe the same structure if they assign the axes differently — and both would be correct. Not all combinations will work, and it is a useful exercise to see how different labels might be related by changing axes. See, for example, whether you can convince yourself that mapping $\mathbf{a}$ to $\mathbf{b}$ to $\mathbf{c}$ back to $\mathbf{a}$ converts $Pnma$ into $Pbnm$. We are not going to worry too much about this in this course, except that it is important to realise that a crystal does not know which axis is $\mathbf{a}$ or $\mathbf{b}$ or $\mathbf{c}$!

We are going to finish this lecture by returning to the andalusite structure shown at the end of BL6. Our task is to decide to which space group this structure belongs. There are various ways of going about this sort of exercise, but the technique we will use here is to find a single atom in the structure that is located on what seems to be a relatively arbitrary

position. So we want to avoid anything that lies on the edge of the unit cell, or exactly half way along, or an atom that appears to lie on a mirror plane etc.

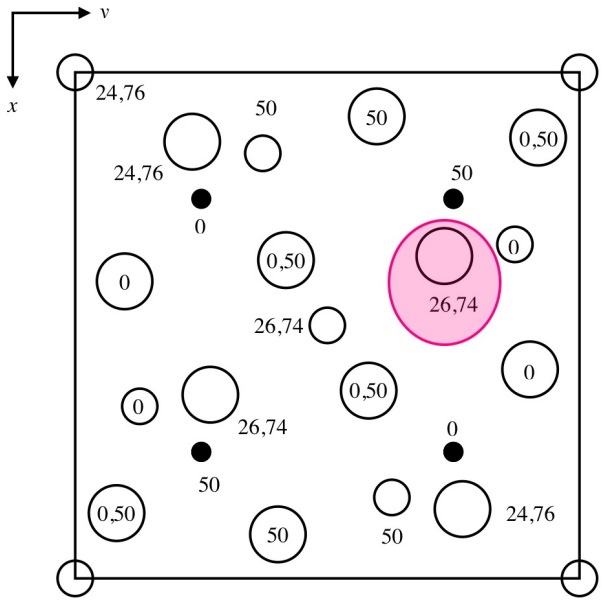

In this particular case, there is an oxygen atom that is located on an arbitrary position. What we are going to do is to treat this oxygen atom as a “general equivalent position” and draw a diagram that shows the positions of all related oxygen atoms within the unit cell.

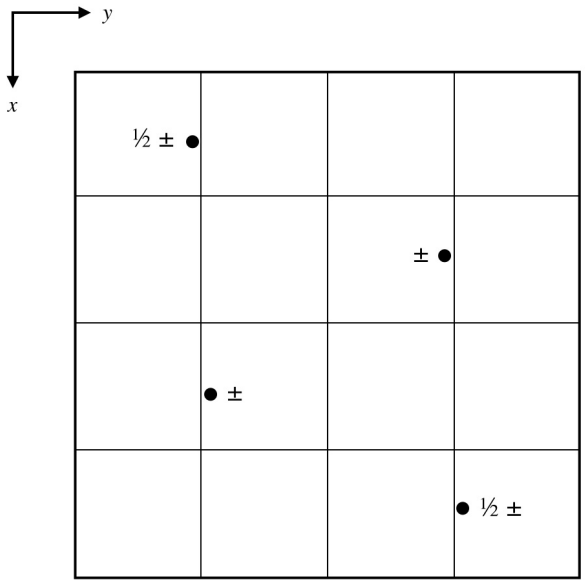

Note that we are not even worried about the absolute coordinates of these atoms, but we are interested in knowing how the position of one atom is related to that of the others. Note also that we have drawn lines at each quarter of a unit cell — this is just to help us with relating positions. The first thing to determine is the lattice centreing. In this case it

is straightforward to see that it is a primitive lattice; hence the first character in the space group symbol is P. Note that we have eight general positions, which for a primitive lattice will mean that the point group must have eight general positions as well. There is only one orthorhombic point group with eight positions: mmm. So already we know that we will have mirror planes or glide planes perpendicular to all three crystal axes.

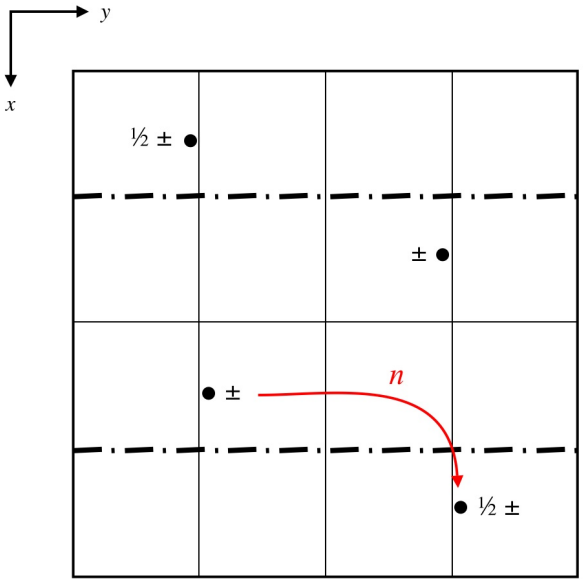

Working systematically, we start with the **a** crystal axis (in this case the axis running vertically along the page), looking for perpendicular mirror planes or glide planes. We know that these will occur either at $x = 0, \frac{1}{2}$ or at $x = \frac{1}{4}, \frac{3}{4}$. So there is no guesswork involved. In this case we find n-glides at $x = \frac{1}{4}, \frac{3}{4}$, and can mark these in on the diagram. The second character of the space group symbol must be n: $Pn--$.

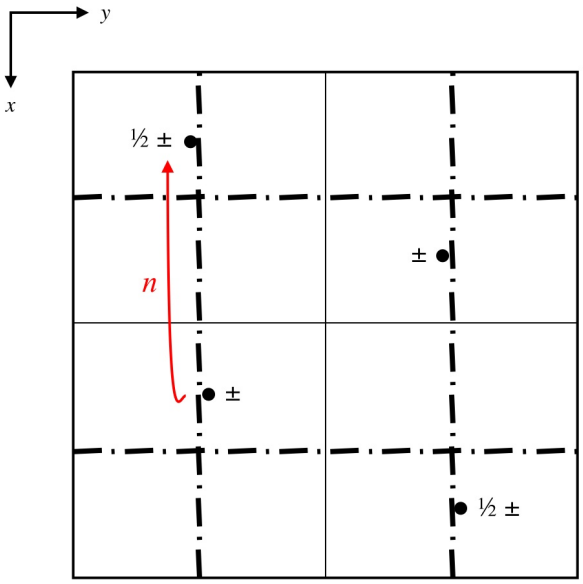

Repeating the process, now for $\mathbf{b}$, we find n-glides perpendicular to $\mathbf{b}$ at $y = \frac{1}{4}, \frac{3}{4}$. So the space group symbol becomes $Pnn-$.

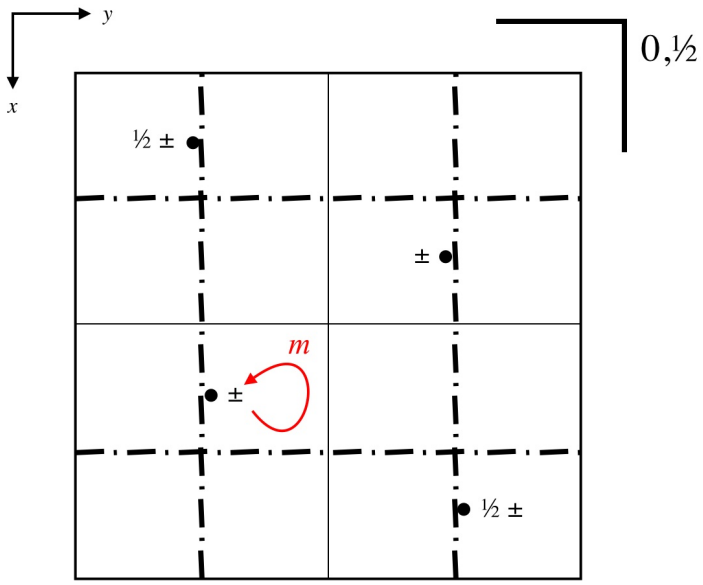

Finally, we look for mirror planes or glide planes perpendicular to $\mathbf{c}$. This is perhaps the easiest operation to spot: we have mirror planes at $z = 0, \frac{1}{2}$. Putting all this information together, we can say that the space group of andalusite is $Pnnm$, its point group is mmm, it is centrosymmetric (can you spot the centres of symmetry?) and its diffraction pattern will have point symmetry mmm. These are the sorts of results you will be expected to be able to obtain given the plan of a crystal structure.

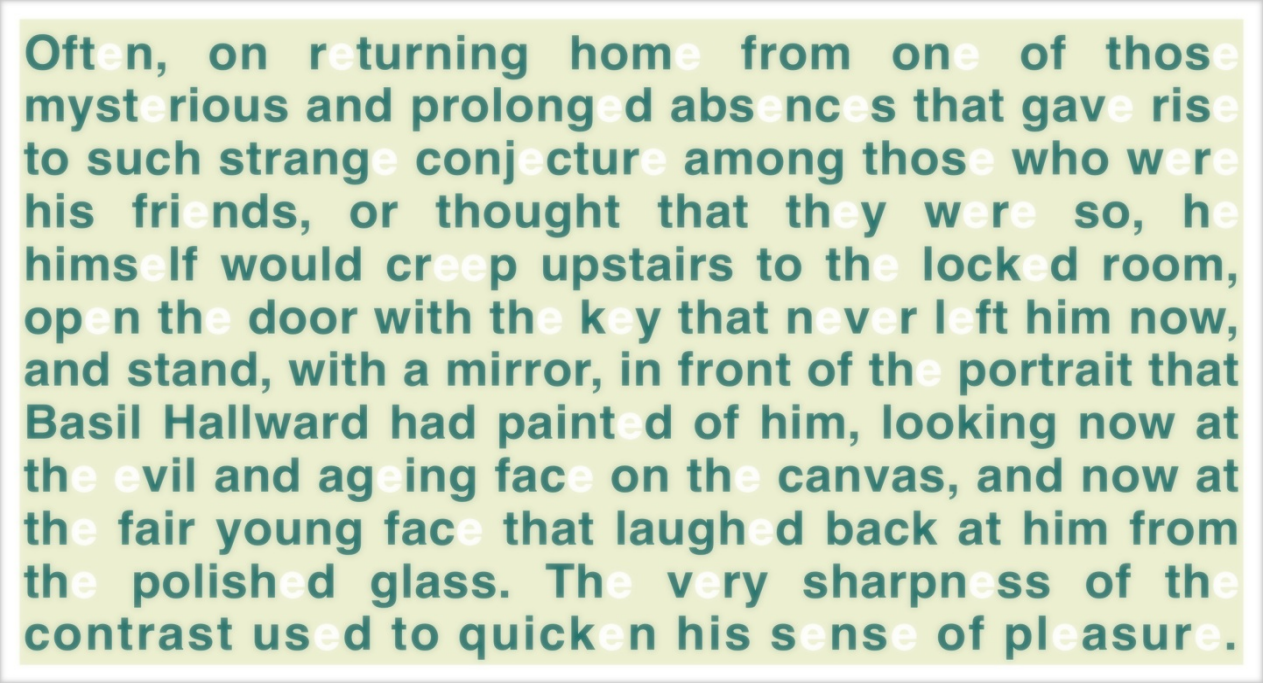

Untitled, Wes Radolič, 1984

BL8: Systematic Absences

We discussed previously the possibility that crystal symmetry might be used to simplify the interpretation of crystallographic experiments. Having formalised what we mean by crystal symmetry, we can revisit this issue by observing how the various symmetry elements — Bravais lattice, translational symmetry and point symmetry — affect diffraction patterns.

Let us begin by reminding ourselves of two key results that we have already shown. The first is known as Friedel's law, and tells us that the structure factors at reciprocal space vectors $\mathbf{Q}$ and $-\mathbf{Q}$ are in fact complex conjugates; *i.e.* $F(hkl) = F^*(\bar{h}\bar{k}\bar{l})$. This means that the corresponding diffraction intensities are equal: $I(hkl) = I(\bar{h}\bar{k}\bar{l})$.

The second key result was that the point symmetry of an object is preserved in its diffraction pattern. When we take into account Friedel's law, this means that the point group of a diffraction pattern is the centrosymmetric parent of the point group of the crystal. You should be able to convince yourself that the diffraction pattern for a crystal in $I4_1cd$ will have $4/mmm$ point symmetry; likewise, that of a crystal in $P6_2$ will have $6/m$ point symmetry.

What we are going to show in this lecture is that the translational symmetry elements do not affect the symmetry of the diffraction pattern *per se*, but do result in what we call "systematic absences" — the absence of any diffraction intensity at specific sets of reciprocal lattice points. Some of this will be familiar from last year's IA course, but it is useful to address this again with our more robust understanding of the diffraction process.

The first type of systematic absences we will address are those that arise due to lattice centreing. Let us consider a face-centred lattice (presumably of orthorhombic or cubic lattice symmetry, but this doesn't matter). What we know is that for each atom j in the unit cell at (x_j, y_j, z_j) there are corresponding atoms j', j'' and j''' at $(x_j, y_j + \frac{1}{2}, z_j + \frac{1}{2})$, $(x_j + \frac{1}{2}, y_j, z_j + \frac{1}{2})$ and $(x_j + \frac{1}{2}, y_j + \frac{1}{2}, z_j)$, respectively. Consequently, we can split our scattering equations into four parts:

$$\begin{aligned} F(hkl) &= \sum_j f_j \Big\{ \exp[2\pi\mathrm{i}(hx_j + ky_j + lz_j)] \\ &\quad + \exp[2\pi\mathrm{i}(hx_j + k\{y_j + \tfrac{1}{2}\} + l\{z_j + \tfrac{1}{2}\})] \\ &\quad + \exp[2\pi\mathrm{i}(h\{x_j + \tfrac{1}{2}\} + ky_j + l\{z_j + \tfrac{1}{2}\})] \\ &\quad + \exp[2\pi\mathrm{i}(h\{x_j + \tfrac{1}{2}\} + k\{y_j + \tfrac{1}{2}\} + lz_j)] \Big\} \end{aligned} \tag{48}$$

On factorising we obtain

$$\begin{aligned} F(hkl) &= \big\{1 + \exp[\pi\mathrm{i}(k + l)] + \exp[\pi\mathrm{i}(h + l)] + \exp[\pi\mathrm{i}(h + k)]\big\} \\ &\quad \times \sum_j f_j \exp[2\pi\mathrm{i}(hx_j + ky_j + lz_j)] \end{aligned} \tag{49}$$

It is not difficult (and a good exercise) to show that the prefactor is zero for all h, k, l except whenever the three indices are all even or are all odd (when it equals four). This means that for a face centred crystal we do not expect to observe any intensity for *e.g.* the (100), (321), ... reflections. Let us use this result to visualise reciprocal space for a face-centred lattice:

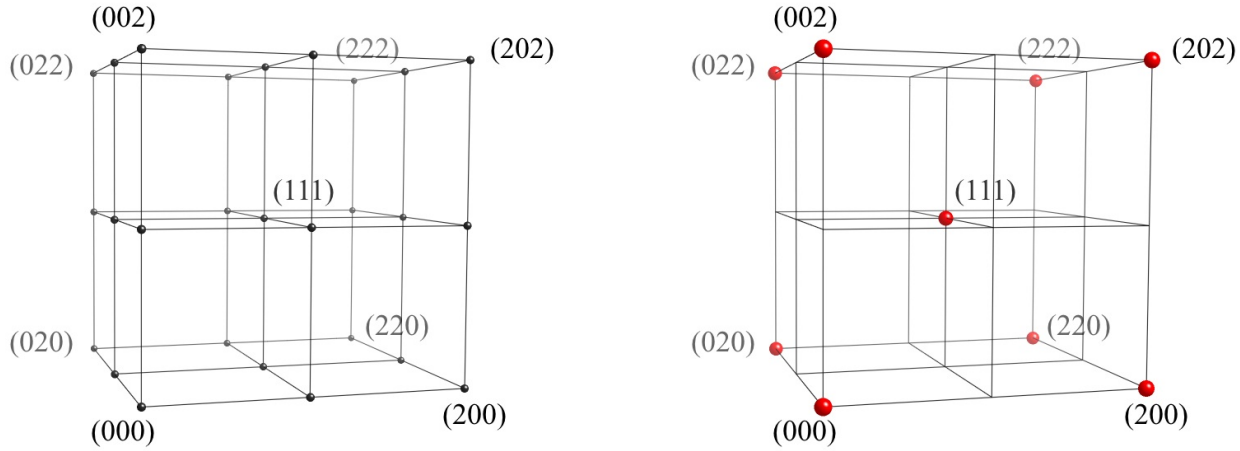

What we find is that the reciprocal lattice of a face-centred cubic lattice is itself a body-centred cubic lattice in reciprocal space. It is a good exercise to check that the reverse

also holds true; that is, to confirm that a body-centred lattice is face-centred in reciprocal space. Consequently, the centreing of a diffraction pattern we observe experimentally will tell us what particular type of centreing exists in real space. This enables us to start determining the space group for our crystal.

The other two translational symmetry operations, namely screw axes and glide planes, also give rise to systematic absences. The mathematics involved is very similar, if a little tedious. We cover some representative derivations here only really to explain from where these results arise; what is important is only that the absences occur, and that we know how to recognise and interpret these in a diffraction pattern.

Let us quickly address the mathematics then for screw axes, and we will use as our example a crystal that contains a 2_1 screw axis parallel to $\mathbf{b}$. This will have the effect of replicating each atom j, originally at (x_j, y_j, z_j), at $(-x_j, \frac{1}{2}+y_j, -z_j)$. The structure factor is then given as

$$F(hkl) = \sum_j f_j \big\{ \exp[2\pi \mathrm{i}(hx_j + ky_j + lz_j)] + \exp[2\pi \mathrm{i}(-hx_j + k\{\tfrac{1}{2} + y_j\} - lz_j)] \big\}. \qquad (50)$$

What we do is to consider the intensity at reciprocal lattice points of the type $(0k0)$:

$$\begin{aligned} F(0k0) &= \sum_j f_j \big\{ \exp(2\pi \mathrm{i} k y_j) + \exp[2\pi \mathrm{i} k(\tfrac{1}{2} + y_j)] \big\} && (51) \\ &= [1 + (-1)^k] \sum_j f_j \exp(2\pi \mathrm{i} k y_j) && (52) \\ \begin{cases} = & 0 \text{ if } k = 2n+1 \quad (\text{odd}) \\ \neq & 0 \text{ if } k = 2n \quad (\text{even}) \end{cases} && (53) \end{aligned},$$

where n is an integer. What this tells us is that $(0k0)$ reflections with odd values of k will not be observed: a new set of "systematic absences" that we should be able to observe in a diffraction pattern. Similar systematic absences would arise from screw axes along other directions.

For completeness we will cover a similar calculation for glide planes. This time our example will be a c-glide perpendicular to $\mathbf{b}$. This will replicate each atom j, originally at (x_j, y_j, z_j), at $(x_j, -y_j, \frac{1}{2}+z_j)$. Writing out the structure factor explicitly we obtain

$$F(hkl) = \sum_j f_j \big\{ \exp[2\pi \mathrm{i}(hx_j + ky_j + lz_j)] + \exp[2\pi \mathrm{i}(hx_j - ky_j + l\{\tfrac{1}{2} + z_j\})] \big\}. \qquad (54)$$

Now, for $(h0l)$ reflections we have

$$F(h0l) = \sum_j f_j\{\exp[2\pi\mathrm{i}(hx_j + lz_j)] + \exp[2\pi\mathrm{i}(hx_j + l\{\tfrac{1}{2} + z_j\})]\} \quad (55)$$

$$= [1 + (-1)^l] \sum_j f_j \exp[2\pi\mathrm{i}(hx_j + lz_j)] \quad (56)$$

$$\begin{cases} = & 0 \text{ if } l = 2n+1 \quad (\text{odd}) \\ \neq & 0 \text{ if } l = 2n \quad (\text{even}) \end{cases}, \quad (57)$$

where again n is an integer. Similar systematic absences arise from glide planes involving other directions.

We can summarise these three types of systematic absences in three separate tables.

Conditions due to lattice centreing:

Centreing	**Reflection condition**	**Reflections involved**
I	$h + k + l = 2n$	
F	h, k, l all even or all odd	
A	$k + l = 2n$	
B	$h + l = 2n$	all reflections
C	$h + k = 2n$	
R (obverse)	$-h + k + l = 3n$	
R (reverse)	$h - k + l = 2n$	

Conditions due to the existence of screw axes:

Screw axis	**Reflection condition**	**Reflections involved**
2_1	h, k or $l = 2n$	
4_2, 6_3	$l = 2n$	$h00$ for axis $\parallel \mathbf{a}$
3_1, 3_2, 6_2, 6_4	$l = 3n$	$0k0$ for axis $\parallel \mathbf{b}$
4_1, 4_3	$l = 4n$	$00l$ for axis $\parallel \mathbf{c}$
6_1, 6_5	$l = 6n$	

Conditions due to the existence of glide planes (*n.b.* this list is not comprehensive for the d-glides):

Glide plane	Reflection condition	Reflections involved
a	$h = 2n$	
b	$k = 2n$	$0kl$ for plane $\perp \mathbf{a}$
c	$l = 2n$	$h0l$ for plane $\perp \mathbf{b}$
n	$h + k,\ k + l$ or $h + l = 2n$	$hk0$ for plane $\perp \mathbf{c}$
d	$h + k,\ k + l$ or $h + l = 4n$	

More important than all this book-keeping is the ability to interpret systematic absences within a diffraction pattern. In order to build up our expertise here what we are going to do is to consider some simplified reflection diagrams. These are illustrations that show what reflections we expect to see in a diffraction pattern (without worrying about the actual intensities). We will only deal with orthorhombic crystals, for which we will encounter three separate planes in reciprocal space — one perpendicular to each of the three crystal axes.

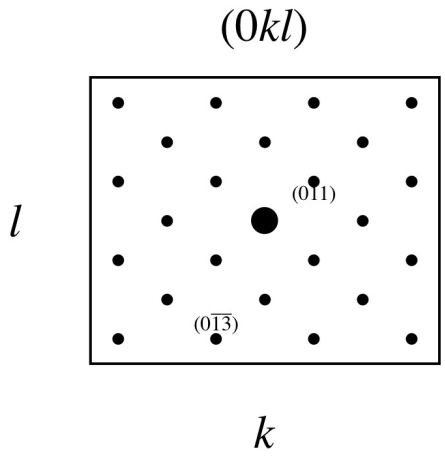

Let us consider the orthorhombic space group $Pnma$. Because we are dealing with a primitive lattice, we do not expect any absences due to lattice centreing. Again, we work systematically, dealing first with the n-glide, which we know lies perpendicular to $\mathbf{a}$. Looking through our table above we see that this this will give rise to absences in the $(0kl)$ reciprocal plane whenever $k + l$ is odd. To represent this we sketch a reflection diagram for the $(0kl)$ plane (above). The central reflection, which is shown as a larger circle, corresponds to (000); k indexes the horizontal axis and l the vertical axis. We draw in smaller circles wherever we expect to see reflections: in this case whenever $k + l$ is even. Two representative points are labelled — (011) and $(0\bar{1}\bar{3})$.

Working systematically we consider the next character in the space group symbol: the m, which tells us we have mirror planes perpendicular to $\mathbf{b}$. There are no systematic absences associated with mirror planes, so we might initially draw a reflection diagram for the $(h0l)$ plane as overleaf. **This is not yet quite correct, and we will see why shortly**.

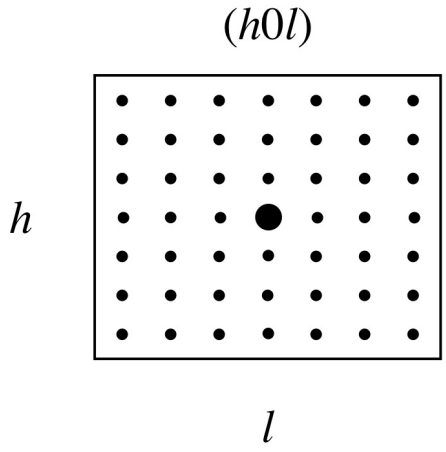

The last character in the space group symbol tells us that we have an a-glide perpendicular to $\mathbf{c}$. Again, consulting our table of reflection conditions, we see that this predicts reflections for the $(hk0)$ plane will only be observed whenever h is even. Transferring this to a reflection diagram, we obtain the following initial guess.

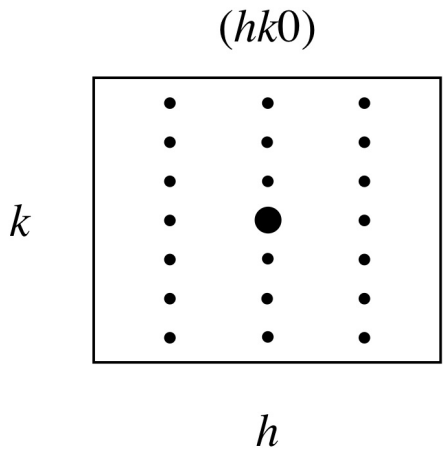

The final — and very important — step is to check for consistency along the three axes $(h00), (0k0), (00l)$. Considering the systematic absences we found for the $(0kl)$ plane, for example, we see that we expect reflections along $(0k0)$ and $(00l)$ only when k or l are even. But this is not yet reflected in the diagrams for $(hk0)$ and $(h0l)$ planes. Similarly, the a-glide absences on $(hk0)$ tell us that we will observe $(h00)$ reflections only when h is even; again we need to represent this on the $(h0l)$ diagram. Putting all this information together, we arrive at the set of reflection diagrams shown on the next page.

It is worth reiterating that the crystal itself does not "know" which axis is which, so the labels themselves are somewhat arbitrary. Here we can label the axes because we are starting from the particular space group symbol $Pnma$. However, if we were to undertake the reverse process — that is, to recover the space group symbol from the scattering

patterns — then we would end up with different, but equivalent, space group symbols for each possible choice of axes.

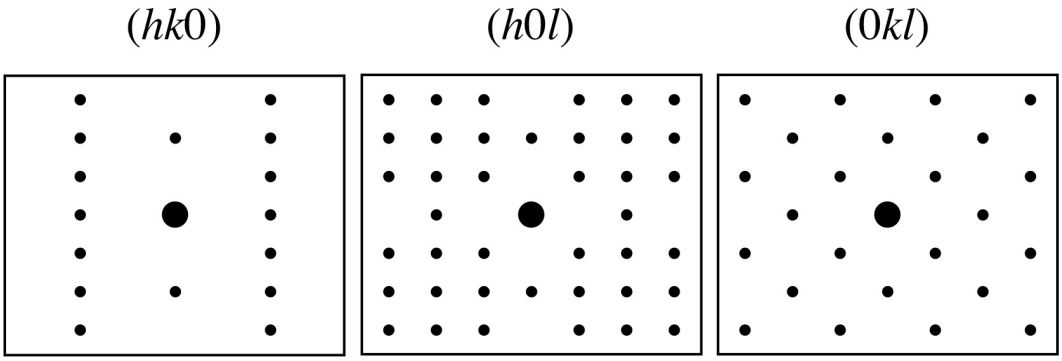

We are going to finish this lecture with a quick discussion of systematic absences in powder diffraction patterns. Because in a powder diffraction experiment we have many small crystallites oriented in all possible directions, what happens is that all of reciprocal space is effectively projected onto a single axis. We can't resolve any directions within reciprocal space but we can still determine magnitudes. An example of a powder diffraction pattern for a face-centred cubic material is shown below. The important point here is to illustrate that we can still see systematic absences; in this case, for example, we could say with confidence that the material is face-centred cubic. The situation becomes more complex for orthorhombic systems, and it may be that not all systematic absences can be determined in this way.

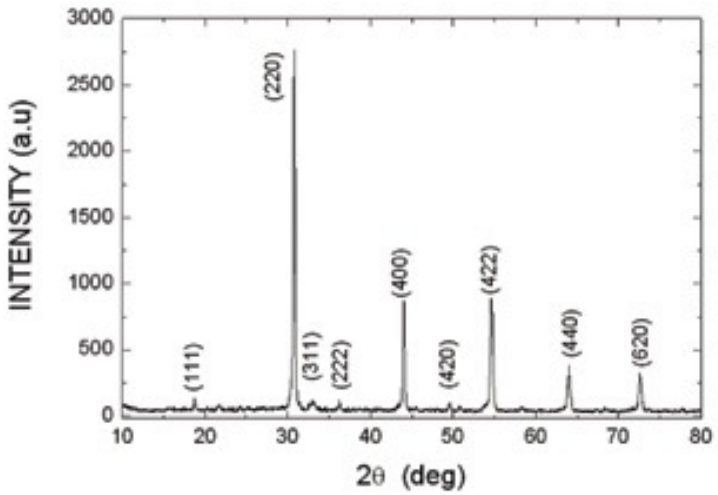

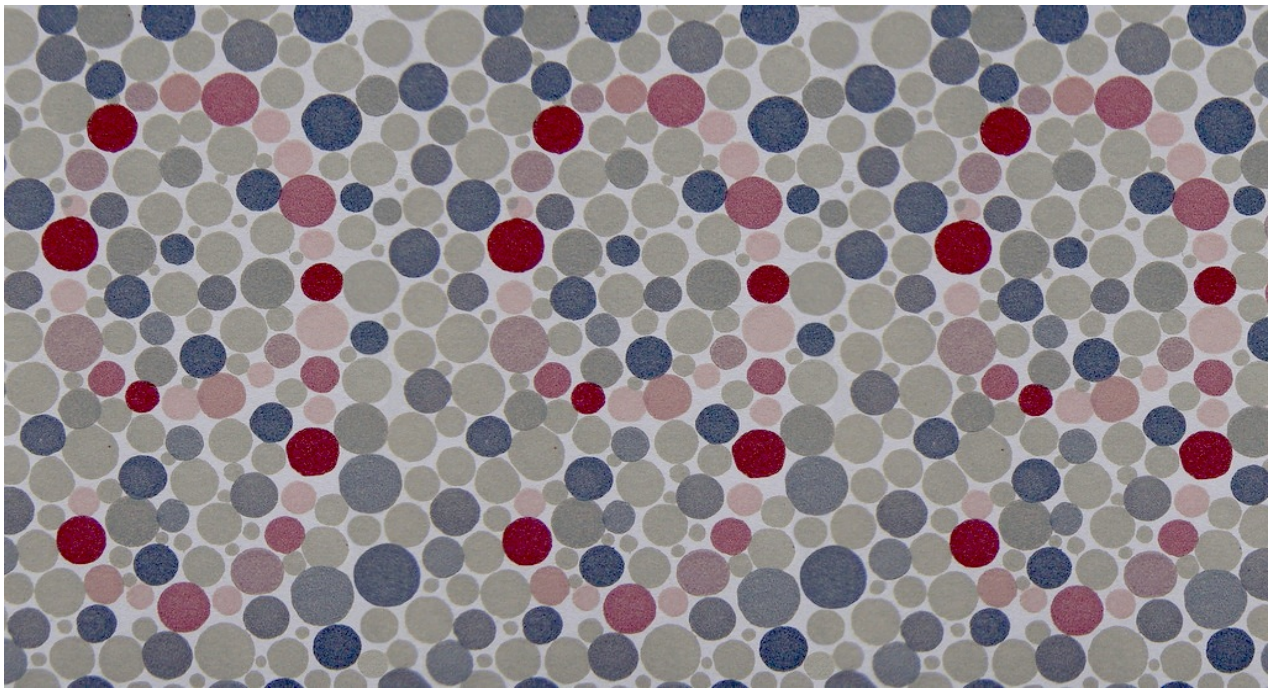

Colorblind?, Flickr:Bansidhe, 2008

BL9: The Phase Problem

The most significant hurdle to be overcome in "solving" a crystal structure from a measured diffraction pattern is the loss of phase information. We measure a quantity related to the magnitude $|F(hkl)|$ of the structure factors but we do not know the complex component that would allow us to recover the values $F(hkl)$ themselves. It is not difficult to see that the phase information is actually very important. We will have covered this in practical sessions, but a good illustration can be provided by returning to our Fourier transforms of cats and ducks.

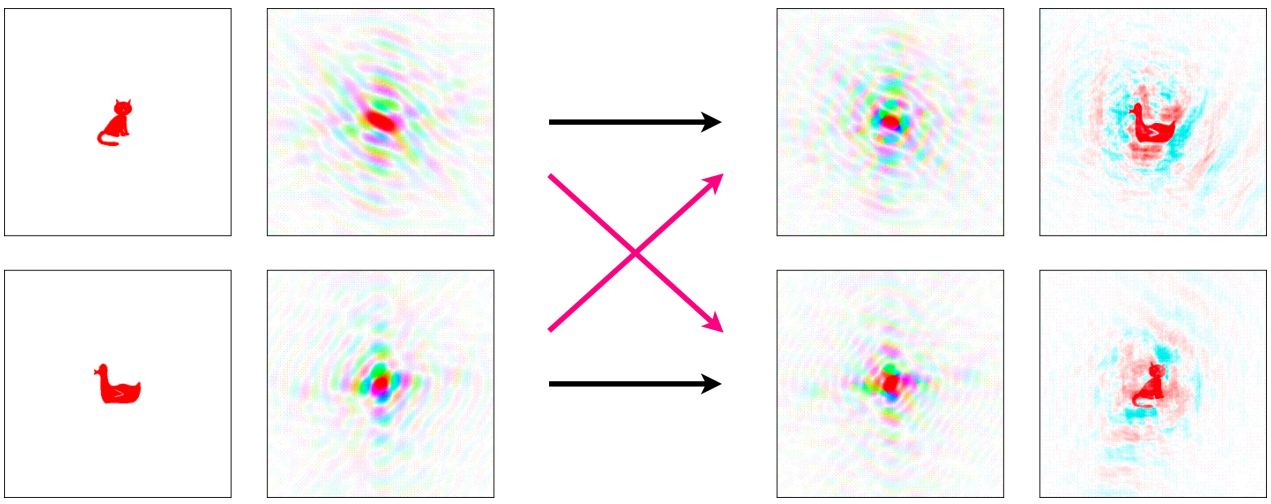

What the picture above shows us is that if we swap the phase information in the Fourier transforms of our two animals, but keep the correct intensities, then when we reconstruct the real-space images via reverse Fourier transform we have essentially swapped the two objects. The information that distinguishes a cat from a duck is contained primarily within the phases, and not the intensities.

We have to work very hard to recover the phase information, and in this lecture we will sketch out the process in broad details. Matters are simplified greatly in centrosymmetric systems because here the phases are all either 0 or π. It is a good exercise to verify this mathematically, but a pictorial explanation will suffice here.

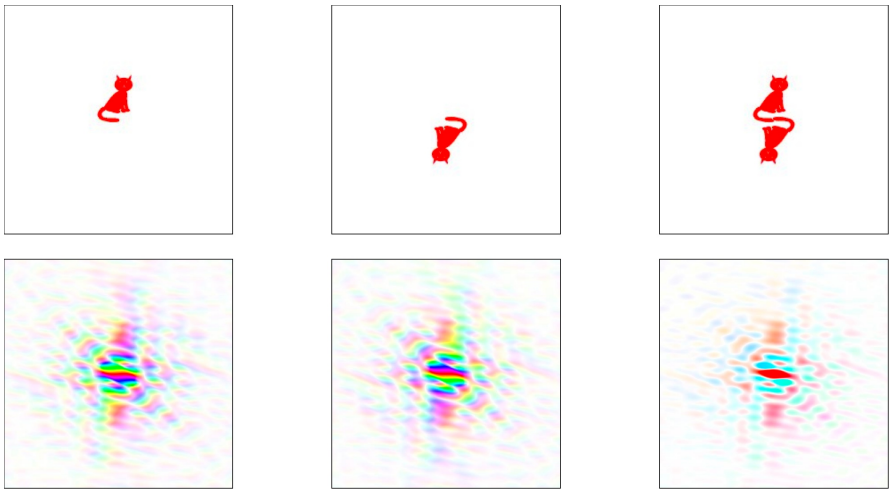

Consider the Fourier transform of a cat (shown again on the left above), and how this Fourier transform changes if we invert the real space image (centre illustration). What we see is that the intensities all remain unchanged, but the phases have been inverted. That is, the Fourier components have undergone complex conjugation. If we add the two pictures in real space to give a centrosymmetric pair of cats, then we also add the corresponding Fourier transforms. The imaginary components cancel exactly, and we are left with phases of either 0 ($F(\mathbf{Q})$ a positive real number) or π ($F(\mathbf{Q})$ a negative real number).

The very first step in solving the structure of a material is to determine the unit cell dimensions. The position of reflections in the diffraction pattern will give us this information, but these need to be calibrated at some point against a standard whose unit cell dimensions are known precisely. Most modern x-ray diffractometers will deduce the unit cell automatically, by arriving at a trial set of lattice parameters from a small number of reflections and then searching for other reflections based on this cell.

Once we know the unit cell dimensions, we can calculate the unit cell volume. Multiplying this value by the known density of the crystal will give us the mass of the atoms in the unit cell. This is important because this enables us to calculate the number of formula units in the unit cell (assigned the symbol Z), and this can help us determine which atoms must lie on high symmetry positions. We will return to this point shortly.

The next task is to determine the point symmetry of the diffraction pattern. This is straightforward and tells us immediately to which Laue class (the centrosymmetric point groups) and hence to which crystal system the crystal belongs.

We then look for systematic absences, checking first for signs of lattice centreing, and then for any indication of the existence of svrew axes and/or glide planes. This will hep to narrow down the choice of space group, but there may not be sufficient information to arrive at a unique answer.

Often it is very useful to know whether the crystal is centrosymmetric or not. Of course the diffraction pattern is always centrosymmetric, but it is possible that systematic absences will give some clue. An example is the acentric space group $P2_12_12_1$ (worth checking).It is also the case that for some systems we may know from certain physical propertes (such as the existence of a piezoelectric response) that the crystal must be acentric.

A more general approach is to make use of so-called "Wilson statistics", which help because centrosymmetric and acentric crystals give rise to two different distributions of diffraction intensities — *irrespective* of the actual system involved. To see how this works we need first to place the diffraction intensities onto a normalised scale — a slightly protracted process whose description requires some patience! We begin by noting that the intensities we measure in a diffraction experiment give us a relative structure factor $F_{\rm rel}(hkl)$ that is related to the real structure factor $F(hkl)$ by some unknown scale factor s:

$$F_{\rm rel}(hkl) = s|F(hkl)| \tag{58}$$

We will need to evaluate s to be able to work out the "true" structure factors. To do this we extract the temperature factor from $F(hkl)$, replacing it by a "motion free" $\tilde{F}(hkl)$:

$$F_{\rm rel}(hkl) = s\exp(-B\sin^2\theta/\lambda^2)|\tilde{F}(hkl)| \tag{59}$$

It can be shown that the average of the $|\tilde{F}(hkl)|^2$ values taken over small ranges in Q is given by the sum of the squared form factors f_j^2:

$$\langle|\tilde{F}(hkl)|^2\rangle = \sum_j f_j^2 \tag{60}$$

Rearranging these equations we arrive at the expression

$$2\ln s - 2B\sin^2\theta/\lambda^2 = \ln K, \tag{61}$$

where

$$K = \frac{\langle F_{\rm rel}^2(hkl)\rangle}{\sum_j f_j^2}. \tag{62}$$

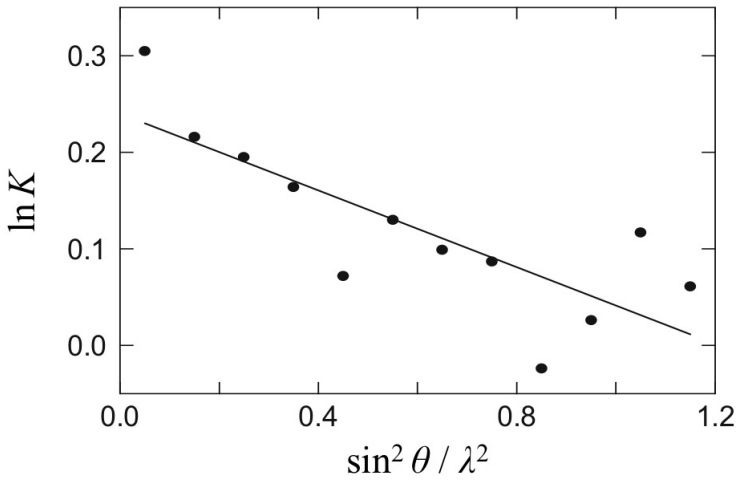

We can calculate K for different regions of Q (and hence $\sin\theta/\lambda$), noting that a plot of $\ln K$ against $\sin^2\theta/\lambda^2$ should give a straight line whose intercept is $2\ln s$, and whose slope is $-2B$. Such a graph is called a "Wilson plot" (after its inventor).

The "normalised structure factors", $E(hkl)$, whose distribution is going to tell us whether the crystal is centrosymmetric or not are obtained by dividing out the form factors from the $\tilde{F}(hkl)$ we have just obtained:

$$|E(hkl)|^2 = \frac{|\tilde{F}(hkl)|^2}{\varepsilon \sum_j f_j^2}, \tag{63}$$

where ε is usually equal to 1 (depending on the point group of the crystal structure, some classes of reflections require larger integral values of ε). The normalised structure factors will have the same phase as the real structure factors. The important point is that the $E(hkl)$ approximate the structure factors for point atoms; that is, if we could take out the spread of electron distribution about each atom position, and also the distribution of atom positions due to thermal motion. Now, what Wilson showed was that if we have done this correctly we should find $\langle E^2\rangle = 1$, and then either one of two possible values for $\langle E\rangle$ and again for $\langle|E^2-1|\rangle$ for centrosymmetric and acentric crystals:

Crystal type	$\langle E^2\rangle$	$\langle E\rangle$	$\langle\|E^2-1\|\rangle$
centrosymmetric	1	$\sqrt{2/\pi} = 0.798$	0.968
acentric	1	$\sqrt{\pi}/2 = 0.886$	0.736

The next stage is to try to assign phases to the normalised structure factors. The traditional idea has been that if the phases of the most intense reflections could be deduced somehow, then these could be used in a Fourier synthesis of the structure. These phases could only be deduced by estimating the positions of some of the atoms, particularly those that scatter the most strongly. There are two approaches that help us here. The first is to

consider the space group symmetry, if it is known at this stage, in the context of the number of formula units per unit cell (Z). For example, if we were to have two sets of orthogonal mirror planes in our space group, then we would end up with different numbers of atoms depending on whether they lay on 0, 1 or 2 mirror planes. It could be that the value of Z dictates which of these must be the case for a given heavy atom.

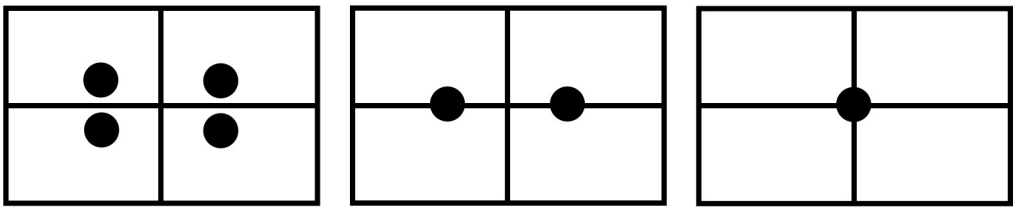

The other technique that is useful at this early stage is to reconstruct a Patterson map (see page BH 27) via reverse Fourier transform of the $|E(hkl)|^2$. This will tell us the key interatomic vectors, and these too might be sufficient to determine some atomic positions when we take into account the space group symmetry.

Once we have assigned the positions of one or two of the most strongly scattering atoms then the structure factors can be calculated using only these few atoms. The phases of the strongest reflections obtained in this calculation can be taken to apply to the measured structure factors and used to give a new Fourier synthesis of the real space distribution. The structure that is obtained may not be complete, but it may show some new atoms. These can then be used to improve the calculation of the phases, bringing in some of the weaker reflections, and the procedure repeated until the positions of all the atoms have been deduced.

An important tool in determining phases for subsequent reflections is to use what is known as "Sayre's equation". In its simplest form for centrosymmetric crystals, it states that if $s(\mathbf{Q})$ is the sign of a given reflection (remember phases in centrosymmetric crystals are $= 0, \pi$) then the phases of three reflections are related by the simple product

$$s(\mathbf{Q}_1) \times s(\mathbf{Q}_2) \times s(\mathbf{Q}_3) \approx +1, \tag{64}$$

whenever the three scattering vectors are related by $\mathbf{Q}_1 + \mathbf{Q}_2 + \mathbf{Q}_3 = 0$. Here the symbol "$\approx$" denotes "probably equal to": this probability can be calculated, and depends on the magnitudes of the E-values of the three reflections. Thus Sayre's equation properly holds only for the strongest reflection. This may be enough to generate the phases of a useful number of reflections, at which stage a stronger version of Sayre's equation can be used:

$$s(\mathbf{Q}) = \sum_{\mathbf{Q}'} s(\mathbf{Q}')s(\mathbf{Q} - \mathbf{Q}'), \tag{65}$$

for which the probability is higher, so that some of the less intense reflections can be used.

Once the phases of a sufficient number of reflections have been determined, an approximate electron density map can be produced by Fourier synthesis. The end result is a set of atomic coordinates. No attempt has been made to pinpoint the positions with any precision, and this will be our final task. Precise coordinates are necessary for the determination of bond lengths and bonding geometries. We may also be interested in the amplitudes of thermal vibrations.

This final stage is referred to as "structure refinement" (the process discussed above is that of "structure solution"). Essentially what we try do in refinement is to vary the positions of atoms and the thermal displacement parameters B so that we obtain a structural model that is capable of reproducing the experimental scattering intensities as accurately as possible. It is common to use a least-squares method to vary these parameters, but for this to work we need to have some measure of the "goodness-of-fit" for a given model. The quantity that is minimised is the difference in observed and calculated absolute structure factors, weighted by the estimated errors involved:

$$\sum_{hkl} \big| |F_{\rm obs}(hkl)| - |F_{\rm calc}(hkl)| \big| / \sigma^2(hkl) \tag{66}$$

Crystallographers commonly use a quantity called the R-factor to asses the final quality of the model:

$$R = 100\% \times \frac{\sum_{hkl} \big| |F_{\rm obs}(hkl)| - |F_{\rm calc}(hkl)| \big|}{\sum_{hkl} |F_{\rm obs}(hkl)|} \tag{67}$$

By comparing the moduli of the structure factors we avoid any problem with the phases. The comparison with the experimental values is direct. A typical value of R for a refined mineral structure will be a few percent for x-ray single crystal data. One would expect to be able to determine absolute atomic positions to within 0.01 Å or better in such a model.

So we come to the end of our course, having achieved our original goal. We have studied how diffraction experiments can be used to determine the atomic-level structure of materials. In the process we have learned about reciprocal space, about symmetry and about diffraction as an experimental technique. What follows are some appendices which give derivations of formulae quoted in the text, a list of Nobel prizes in crystallography and a glossary of terms for quick reference.

Appendix: Convolution theorem

We say that the function $f(x)$ is the convolution of two functions $g(x)$ and $h(x)$ if

$$f(x) = \int g(x')h(x - x')\,\mathrm{d}x'. \tag{68}$$

We denote this relationship as $f(x) = g(x) \otimes h(x)$ (an alternative representation sometimes used is $f = g * h$). The convolution is essentially an integral that expresses the amount of overlap of the function $h(x)$ as it is shifted over the function $g(x)$: it essentially "blends" one function with another.

The operation is commutative:

$$\begin{aligned}
g(x) \otimes h(x) &= \int_{-\infty}^{\infty} g(x')h(x - x')\,\mathrm{d}x' \\
&= \int_{\infty}^{-\infty} g(x - x'')h(x'') \cdot -\mathrm{d}x'' \qquad (x'' = x - x') && (69)\\
&= \int_{-\infty}^{\infty} h(x'')g(x - x'')\,\mathrm{d}x'' && (70)\\
&= h(x) \otimes g(x) && (71)
\end{aligned}$$

Our key result actually concerns the Fourier transform of a convolution. Writing the transforms of our three functions $f(x)$, $g(x)$ and $h(x)$ as $F(k)$, $G(k)$ and $H(k)$, respectively, we have:

$$\begin{aligned}
F(k) &= \int f(x)\exp(\mathrm{i}kx))\,\mathrm{d}x && (72)\\
&= \int g(x) \otimes h(x)\exp(\mathrm{i}kx)\,\mathrm{d}x && (73)\\
&= \iint g(x')h(x - x')\exp(\mathrm{i}kx)\,\mathrm{d}x'\,\mathrm{d}x && (74)\\
&= \iint g(x')h(x - x')\exp[\mathrm{i}k(x - x')]\exp(\mathrm{i}kx')\,\mathrm{d}x'\,\mathrm{d}x && (75)\\
&= \int g(x')\exp(\mathrm{i}kx')\,\mathrm{d}x' \times \int h(x - x')\exp[\mathrm{i}k(x - x')]\,\mathrm{d}x && (76)\\
&= \int g(x')\exp(\mathrm{i}kx')\,\mathrm{d}x' \times \int h(x'')\exp(\mathrm{i}kx'')\,\mathrm{d}x'' \qquad (x'' = x - x') && (77)\\
&= G(k) \times H(k) && (78)
\end{aligned}$$

Appendix: Reciprocal lattice derivation

Here we want to show that the Fourier transform of the one-dimensional lattice function $\mathcal{L}(x) = \sum_n \delta(x - na)$ is given by the reciprocal lattice function $\mathcal{R}(Q) = \sum_Q \delta(Q - 2\pi h/a)$. Let us define $\mathcal{R}(Q)$ as the Fourier transform of $\mathcal{L}(x)$. Then we have:

$$\begin{aligned} \mathcal{R}(Q) &= \int \mathcal{L}(x) \exp(\mathrm{i}Qx)\,\mathrm{d}x && (79)\\ &= \int \sum_n \delta(x - na) \exp(\mathrm{i}Qx)\,\mathrm{d}x && (80)\\ &= \sum_n \int \delta(x - na) \exp(\mathrm{i}Qx)\,\mathrm{d}x && (81) \end{aligned}$$

Now, for each integral within the sum on the right-hand side of this equation we will partition space into two regions: that region such that x is less than a small distance ε from na, and all remaining values of x. That is,

$$\begin{aligned} \mathcal{R}(Q) &= \sum_n \left[\int_{|x-na|=\varepsilon}^{\infty} \delta(x - na) \exp(\mathrm{i}Qx)\,\mathrm{d}x \right.\\ &= \left. + \int_{|x-na|=0}^{|x-na|=\varepsilon} \delta(x - na) \exp(\mathrm{i}Qx)\,\mathrm{d}x \right] && (82)\\ &= \sum_n [0 + \exp(\mathrm{i}Qna)] && (83) \end{aligned}$$

Now, for most Q, the summation on the right hand side will cancel over all values of n to give 0. The exception occurs whenever $Q = 2\pi h/a$ (h an integer), in which case

$$\mathcal{R}(Q) = \mathcal{R}(h) = \sum_n \exp(2\pi \mathrm{i}nh) \rightarrow \infty \qquad (84)$$

So $\mathcal{R}(Q)$ is a series of spikes located at $Q = 2\pi h/a$; that is

$$\mathcal{R}(Q) = \sum_h \delta(Q - 2\pi h/a) \qquad (85)$$

as required.

Extending this to three dimensions we have $\mathcal{L}(\mathbf{r}) = \sum_{UVW} \delta[\mathbf{r} - (U\mathbf{a} + V\mathbf{b} + W\mathbf{c})]$. Its Fourier transform is

$$\mathcal{R}(\mathbf{Q}) = \int \mathcal{L}(\mathbf{r}) \exp(\mathrm{i}\mathbf{Q} \cdot \mathbf{r}) \, \mathrm{d}\mathbf{r} \tag{86}$$

$$= \sum_{UVW} \exp[\mathrm{i}\mathbf{Q} \cdot (U\mathbf{a} + V\mathbf{b} + W\mathbf{c})] \tag{87}$$

This function is now a three-dimensional set of δ-functions located at $\mathbf{Q}$ for which $\mathbf{Q} \cdot (U\mathbf{a} + \mathbf{b} + \mathbf{c})$ is an integral multiple of 2π. Consider the vector

$$\mathbf{a}^* = 2\pi \frac{\mathbf{b} \times \mathbf{c}}{\mathbf{a} \cdot (\mathbf{b} \times \mathbf{c})} \tag{88}$$

Note that $\mathbf{b} \times \mathbf{c}$ is a vector perpendicular to both $\mathbf{b}$ and $\mathbf{c}$ so that $\mathbf{a}^* \cdot \mathbf{b} = \mathbf{a}^* \cdot \mathbf{c} = 0$ and

$$\mathbf{a}^* \cdot \mathbf{a} = 2\pi \frac{\mathbf{a} \cdot (\mathbf{b} \times \mathbf{c})}{\mathbf{a} \cdot (\mathbf{b} \times \mathbf{c})} = 2\pi \tag{89}$$

So $\mathbf{Q} = h\mathbf{a}^*$ will satisfy the δ-function requirement for all integral h. Similarly, assigning

$$\mathbf{b}^* = 2\pi \frac{\mathbf{c} \times \mathbf{a}}{\mathbf{b} \cdot (\mathbf{c} \times \mathbf{a})} \tag{90}$$

and

$$\mathbf{c}^* = 2\pi \frac{\mathbf{a} \times \mathbf{b}}{\mathbf{c} \cdot (\mathbf{a} \times \mathbf{b})} \tag{91}$$

means that any integral combination $\mathbf{Q} = h\mathbf{a}^* + k\mathbf{b}^* + l\mathbf{c}^*$ will also satisfy the requirements, giving

$$\mathcal{R}(\mathbf{Q}) = \sum_{hkl} \delta[\mathbf{Q} - (h\mathbf{a}^* + k\mathbf{b}^* + l\mathbf{c}^*)] \tag{92}$$

as required.

Appendix: Nobel Prizes for Crystallography

1901	Roentgen, who discovered X-rays.
1914	von Laue, who discovered the diffraction of X-rays from crystals.
1915	The Braggs—father and son—who developed X-ray diffraction methods for the solution of some simple crystal structures.
1917	Barkla, for his work on the scattering of X-rays from atoms.
1937	Davisson and Germer, who discovered the diffraction of electrons from crystals.
1962	Kendrew and Perutz, for the determination of the crystal structure of hemoproteins.
1962	Crick, Watson and Wilkins, for the structure of DNA.
1964	Hodgkin, for the determination of the crystal structure of vitamin B_{12}.
1982	Klug, for developments in electron microscopy.
1985	Hauptman and Karle, for the development of statistical methods to solve the phase problem in crystallography (direct methods).
1986	Ruska, for developments in electron microscopy, and Rohrer and Binning, for the invention of scanning tunnelling microscopy.
1994	Schull and Brockhouse, for developments in neutron scattering methods.
1997	Walker, for the determination of the crystal structure of ATP Synthase.

Glossary of terms

Acentric structure: Structure that does not have a centre of symmetry.

Atomic scattering factor: Gives the amplitude of a wave scattering from an atom for a given value of $\mathbf{Q}$. For X-rays scattered from the electrons in an atom, the atomic scattering factor decreases with increasing $\mathbf{Q}$ in a way determined by the distribution of electrons.

Centred lattice: Lattice that can be described with orthogonal axes and lattice points on the centres of faces or in the centre of the unit cell.

Centrosymmetric structure: Structure that has a centre of symmetry.

Convolution: The operation of merging two functions such that every part of one function is replaced by a copy of the second function with weight given by the first function.

Debye-Waller factor: Gives a decrease in the amplitude of a diffracted beam of radiation due to the thermal motions of atoms. Alternatively called the *temperature factor*.

Diffuse scattering: Scattering of a beam of radiation from a crystal in addition to the normal Bragg diffraction. Diffuse scattering is not restricted to scattering vectors that are reciprocal lattice vectors. The part of a diffracted beam that is lost due to thermal motion is scattered as diffuse scattering.

Dirac delta function: Function defined by a spike with zero width and integral of 1. Is useful as a means of describing the positions of particles.

Direct methods: Methods used to determine the phases of structure factors based on statistical analysis of the measured magnitudes of the structure factors.

Fourier series: Decomposition of a periodic function into a set of waves which can be combined to reconstruct the function.

Fourier synthesis: Combination of Fourier waves to construct the original function. This term is often used to denote the combination of structure factors to construct the electron density of a crystal.

Fourier transform: Decomposition of a non-periodic function into a set of waves which can be combined to reconstruct the function. The Fourier transform contains the complex amplitudes of all the waves that can be combined to reconstruct the function.

Friedel's law: States that the intensities of reflections (hkl) and $(\bar{h}\bar{k}\bar{l})$ will be equal.

Gaussian function: Symmetric function of the form $f(x) = \exp(-x^2)$.

General equivalent positions: Equivalent positions in the unit cell generated by the symmetry of the crystal. The general equivalent positions do not lie on positions with special symmetry.

Glide symmetry: Symmetry that combines a reflection of the object in a plane (called the *glide plane*) with a translation along the direction of a lattice vector by half the lattice repeat.

Laue symmetry: Symmetry of the diffraction pattern of the crystal. The Laue symmetry is formed by combining the point symmetry of the crystal with a centre of symmetry.

Neutron diffraction: Diffraction of a beam of neutrons by a crystal. The neutrons are diffracted by the atomic nuclei rather than the electrons.

Normalised structure factor: Structure factor corresponding to a crystal containing point atoms with no thermal motion. The normalised structure factor can be obtained from experimental measurements by dividing the atomic scattering factors and the temperature factor—this is equivalent to deconvoluting the effects of atom size and thermal motion.

Oscillation camera: X-ray camera in which the film is wrapped in a cylinder about the crystal, and the crystal rotates about the axis of the cylinder. The beam of X-rays strike the crystal from a direction normal to the axis of oscillation.

Pair distribution function: Function that gives the distribution of distance between atoms.

Patterson method: Fourier transform of the set of measured diffraction intensities. The result is a map of all interatomic vectors. The Patterson map can be useful for identifying the relative positions of atoms which scatter a beam of radiation most strongly.

Phase of a wave: Angular position of the maximum of a wave relative to some origin.

Phase problem: The inherent problem in experimental diffraction by which the phases of the structure factors cannot be measured.

Point group: Combination of symmetry elements that operate on a point (rotation and rotoinversion axes, mirror planes, centre of symmetry). Contrast with *space group*.

Point group symbol: Symbol that contains information about the symmetry in a given point group.

Point particle: Particle with no size. The atomic nucleus is effectively a point particle since its size cannot be resolved by neutron diffraction.

Precession camera: Camera that uses a complex precession motion of the crystal and film to record an undistorted section of reciprocal space.

Primitive lattice: Lattice with only one lattice point contained in the unit cell (contrast with *centred lattice*).

Radial distribution function: See *pair distribution function*.

Resolution: Limit to which features can be determined in a function that has been reconstructed from experimental data.

Scattering vector: Vector that represents the change in wave-vector of a diffracted beam of radiation, given symbol $\mathbf{Q}$. For diffraction of a beam of fixed wavelength λ, $|\mathbf{Q}| = 4\pi \sin\theta/\lambda$.

Screw symmetry: Symmetry that combines a rotation of the object about an axis parallel to a lattice vector (called the *screw axis*) with a translation along the direction of the vector by some fraction of the lattice repeat.

Sinc function: Function of the form $\sin(x)/x$.

Space group: Combination of crystal symmetry elements, including point symmetry and translational symmetry (lattice; rotation, rotoinversion and screw axes; mirror and glide planes; centre of symmetry). Contrast with *point group*.

Space group symbol: Symbol that contains information about the symmetry in a given space group.

Special equivalent positions: Set of positions of special symmetry in a unit cell that are related by all the symmetry operations of the crystal. The set may involve points on mirror planes, rotation and rotoinversion axes, and centres of symmetry.

Structure factor: Fourier transform of the crystal for a given reciprocal lattice vector.

Systematic absence: Bragg reflection that has zero intensity because of the symmetry of the crystal.

Temperature factor: See *Debye-Waller factor*.

Wave-vector: Vector that defines the direction and wavelength of a wave. The wave-vector $\mathbf{k}$ is parallel to the direction in which a wave is travelling, and $|\mathbf{k}| = 2\pi/\lambda$.

Wilson plot: Plot of distribution of normalised structure factors in such a way that the slope and intercept of a straight line fitted through the plot gives information about the scale factor and temperature factor.

Wilson statistics: Statistical analysis of the distribution of normalised structure factors that reflects whether the crystal has a centre of symmetry.